Load Restoration and Energy Management of a Microgrid with Distributed Energy Resources and Electric Vehicles Participation under a Two-Stage Stochastic Framework

Hamidreza Momen[1], Ahad Abessi[1], Shahram Jadid[1], Miadreza Shafie-khah[2], João P. S. Catalão[3,*]

[1]*Department of Electrical Engineering, Iran University of Science and Technology, Tehran, Iran*

[2]*School of Technology and Innovations, University of Vaasa, Vaasa, Finland*

[3]*Faculty of Engineering of University of Porto and INESC TEC, Porto, Portugal*

[*] *catalao@fe.up.pt*

Abstract

Natural disasters in recent years have highlighted the need for enhancing the resilience of the power systems against these events. Dynamic microgrid (MG) formation using distributed energy resources (DERs) is the common approach in restoring the critical loads (CLs). On the other hand, vehicle-to-grid (V2G) and grid-to-vehicle (G2V) capabilities in electric vehicles (EVs), as well as the presence of high-powered engine-generators (EGs) embedded in plug-in hybrid electric vehicles (PHEVs) provide a new capability for using electric and fossil energy stored in EVs simultaneously to restore the CLs during an outage. In this regard, the outage management system (OMS) cooperates with aggregators and uses EVs in the form of a public parking lot (PL) or residential parking (RP), besides other resources such as diesel generators and photovoltaic (PV) units. The approach presented in this paper shows the procedure of load restoration and energy management of available resources under a two-stage stochastic framework. Also, a new method is introduced for restoring CLs in the mesh network by using the load control and the master-slave control techniques. The problem is formulated as mixed-integer linear programming (MILP), and simulations are performed on IEEE 123-buses test system and a real distribution network.

Keywords: Load Restoration; Energy Management; Microgrid; Distributed Energy Resources; Electric Vehicles.

Nomenclature

Indices

t	Index of the timeslots
i,j	Index of the network nodes
α	Index of the restored paths
e	Index of the EVs
l	Index of the load control blocks
m	Index of the nodes which master unit located on them
ω	Index of reduced set of the scenarios

Sets

T	Set of the timeslots
N	Set of the network nodes
N_{master}	Set of the nodes, which master unit located on them
N_{loop}	Set of the nodes in potential loop
$N_{\text{loop}_{\text{-DER}}}$	Set of the nodes in potential loop, which master units located on them
N_{slave}	Set of the nodes, which slave units located on them
$N^{i}_{m,children}$	Set of the children nodes of node i, which can be restored by unit m in the radial part
$N^{i,\alpha}_{m,children}$	Set of the children nodes of node i, which can be restored by unit m along path α, in the mesh part
$N^{i,\alpha}_{m,parent}$	Set of the parent nodes of node i, along path α, which restored by unit m
$N^{i}_{m,common}$	Set of the common children nodes of node i, which can be restored by unit m in the mesh part
$\aleph_{m,i}$	Set of the restoration paths of node i, by unit m
$M_{EV,i}$	Set of the available EVs in node i
$M_{EG,i}$	Set of the available EGs in node i
Ω	Set of all reduced scenarios

Variables

l_i	Binary variable, that indicates the restoration status of the load which located on node i
s_i	Binary variable, that indicates the participation status of the slave unit which located on node i
α_i^m	Binary variable, which indicates the restoration status of node i by unit m
$\beta_{i,\alpha}^m$	Binary variable, which indicates the restoration status of node i by unit m and along path α
$\rho_{l,i}^{s,t}$	Binary variable, which specifies the scheduling status of load control block l in node i
$\rho_{l.i}^{\omega,t}$	Binary variable, which specifies the operating status of the load control block l in the node i and scenario ω
$n_{e,i}^{s,t,ch}$	Binary variable, which indicates the scheduled charging status of the EV e in the node i
$n_{e,i}^{s,t,dch}$	Binary variable, which indicates the scheduled discharging status of the EV e in node i
$n_{e,i}^{\omega,t,ch}$	Binary variable, which indicates the operating charging status of the EV e in the node i and scenario ω
$n_{e,i}^{\omega,t,dch}$	Binary variable, which indicates the operating discharging status of the EV e in the node i and scenario ω
$y_{i,e}^{s,t}$	Binary variable, which indicates the scheduled status of the EG e on or off status, in the node i
$y_{i,e}^{\omega,t}$	Binary variable, which indicates the operating of the EG e on or off status, in the node i and scenario ω
$P_{DG,m}^{s,t}$	Scheduled generation power of the DG m
$P_{PV,i}^{s,t}$	Scheduled active power of PV, in the node i
$P_{PV,i}^{\omega,t}$	Operating active power of PV, in the node i and scenario ω
$P_{EVP,i}^{s,ch,t}$	Scheduled charging power of the EV e, in node i
$P_{EVP,i}^{\omega,ch,t}$	Operating charging power of the EV e, in the node i and scenario ω
$P_{EVP,i}^{s,dch,t}$	Scheduled charging power of the EV e, in the node i
$P_{EVP,i}^{\omega,dch,t}$	Operating discharging power of the EV e, in the node i and scenario ω
$P_{PHEV,i}^{s,dch,t}$	Scheduled generation power of the EG e, in the node i
$P_{PHEV,i}^{\omega,dch,t}$	Operating generation power of the EG e, in the node i and scenario ω
$P_{SUP,i}^{s,t}$	Scheduled supplied load in the node i
$P_{SUP,i}^{\omega,t}$	Operating supplied load in the node i and scenario ω
$Q_{PV,i}^{\omega,t}$	Operating reactive power of PV, in the node i and scenario ω

$Q_{EVP,i}^{\omega,ch,t}$	Operating reactive power consumption of the EV parking, in the node *i* and scenario ω
$Q_{EVP,i}^{\omega,dch,t}$	Operating reactive power generation of the EV parking, in the node *i* and scenario ω
$Q_{PHEV,i}^{\omega,dch,t}$	Operating reactive power generation of the EGs, in the node *i* and scenario ω
$Q_{SUP,i}^{\omega,t}$	Operating reactive power consumption, in the node *i* and scenario ω
$p_i^{m,\omega,t}$	Operating active power injected into the node *i*, in scenario ω
$q_i^{m,\omega,t}$	Operating reactive power injected into the node *i*, in scenario ω
$V_i^{m,\omega,t}$	Operating voltage of the node *i*, in the scenario ω
$p_{i,\alpha}^{m,\omega,t}$	Operating active power injected into the node *i* along path α, in scenario ω
$q_{i,\alpha}^{m,\omega,t}$	Operating reactive power injected into the node *i* along path α, in scenario ω
$V_{i,\alpha}^{m,\omega,t}$	Operating voltage of the node *i* along path α, in scenario ω
$\tau_i^{m,p,\omega,t}$	The additional active power calculated in the node *i*, which restored by the DG *m,* in scenario ω
$\tau_i^{m,q,\omega,t}$	The additional reactive power calculated in the node *i*, which restored by the DG *m,* in scenario ω
$p_{e,i}^{s,t,ch}$	Scheduled charging power of the EV *e*, in the node *i* and in scenario ω
$p_{e,i}^{\omega,t,ch}$	Operating charging power of the EV *e*, in the node *i* and scenario ω
$p_{e,i}^{s,t,dch}$	Scheduled discharging power of the EV *e*, in the node *i* and scenario ω
$p_{e,i}^{\omega,t,dch}$	Operating discharging power of the EV *e*, in the node *i* and scenario ω
$SOC_{e,i}^{s,t}$	Scheduled SOC of the EV *e*, in the node *i* and scenario ω
$SOC_{e,i}^{\omega,t}$	Operating SOC of the EV *e*, in the node *i* and scenario ω
$p_{e,i}^{EG,s,t}$	Scheduled generation power of the EG *e*, in the node *i* and scenario ω
$p_{e,i}^{EG,\omega,t}$	Operating generation power of the EG *e*, in node *i* and scenario ω
$g_{i,e}^{s,t}$	Scheduled fuel consumption of the EG *e*, in the node *i* and in scenario ω
$g_{i,e}^{\omega,t}$	Operating fuel consumption of the EG *e*, in the node *i* and in scenario ω
$g_{z,i,e}^{s,t}$	Scheduled z^{th} section of linearized fuel consumption function of the EG *e*, in the node *i* and in scenario ω
$g_{z,i,e}^{\omega,t}$	Operating z^{th} section of linearized fuel consumption function of the EG *e*, in the node *i* and in scenario ω

Constants and parameters

$P_{critical,i}^{s,t}$	Expected active load consumption in the node *i*
$P_{critical,i}^{\omega,t}$	Active load consumed in the node *i* and in scenario ω
$Q_{critical,i}^{\omega,t}$	Reactive load consumed in the node *i* and in scenario ω
$P_{control,i}^{s,t,l}$	Expected amount of the load control block in the node *i*
$P_{control,i}^{\omega,t,l}$	The amount of the load control block in the node *i* and in scenario ω
r_{ij}	Resistance between the nodes *i* and *j*
x_{ij}	Reactance between the nodes *i* and *j*
V_0^m	Rated voltage of the network
CAP^m	Capacity of the DG *m*
p_m^{max}	Maximum active power generation of the DG *m*
q_m^{max}	Maximum reactive power generation of the DG *m*
$P_{PV,i}^{max,s,t}$	Expected maximum active power generation of PV in the node *i*
$P_{PV,i}^{max,\omega,t}$	maximum active power generation of PV in the node *i* and in scenario ω
$Q_{PV,i}^{max,\omega,t}$	maximum reactive power generation of PV, in node *i* and in scenario ω
$p_{e,i}^{s,ch,max}$	Expected maximum charging power of EV *e*, in node *i*
$p_{e,i}^{\omega,ch,max}$	maximum charging power of EV *e*, in node *i* and scenario ω
$p_{e,i}^{s,dch,max}$	Expected maximum discharging power of the EV *e*, in the node *i*
$p_{e,i}^{\omega,dch,max}$	maximum charging power of the EV *e*, in the node *i* and scenario ω
$SOC_{e,i}^{s,ini}$	Expected initial SOC of the EV *e,* in the node *i*
$SOC_{e,i}^{s,des}$	Expected desired SOC of the EV *e,* in the node *i*
$SOC_{e,i}^{\omega,ini}$	Initial SOC of the EV *e,* in the node *i* and scenario ω
$SOC_{e,i}^{\omega,des}$	Desired SOC of the EV *e,* in the node *i* and scenario ω

$SOC_{e,i}^{s,min}$	Expected minimum SOC of the EV *e*, in the node *i*
$SOC_{e,i}^{s,max}$	Expected maximum SOC of the EV *e,* in the node *i*
$SOC_{e,i}^{\omega,min}$	Minimum SOC of the EV *e,* in the node *i* and scenario ω
$SOC_{e,i}^{\omega,max}$	Maximum SOC of EV *e,* in node *i* and scenario ω
$g_{i,e}^{s,min}$	Expected minimum rate of fuel consumption of the EG *e* in the node *i*
$g_{i,e}^{\omega,min}$	Minimum rate of fuel consumption of the EG *e,* in the node *i* and scenario ω
$g_{i,e}^{s,max}$	Expected maximum rate of fuel consumption of the EG *e* in the node *i*
$g_{i,e}^{\omega,max}$	Maximum rate of fuel consumption of the EG *e,* in the node *i* and scenario ω
$g_{i,e}^{s,fix}$	Expected fixed fuel consumption of the EG *e*, in the node *i*
$g_{i,e}^{\omega,fix}$	Fixed fuel consumption of the EG *e*, in the node *i* and scenario ω
$FR_{e,i}^{initial}$	Initial fuel of the EG *e*, in the node *i*
$FR_{e,i}^{min}$	Minimum fuel remaining in the EG *e*, in the node *i*
η^{ch}	Charging efficiency of all EVs
η^{dch}	Discharging efficiency of all EVs
T_{arr}	Expected arrival time of the EV
t_{arr}	Arrival time of the EV
T_{dep}	Expected departure time of the EV
t_{dep}	Departure time of the EV
t_{rs}	Outage start time
t_{re}	Outage end time

1. Introduction

Because of climate change, the number and severity of natural disasters, such as earthquakes and storms have increased. These events have caused much damage to the power system [1]. For example, since 2002, weather-related incidents in the United States (US) have caused about 80 percent of the blackouts, which have included a population of more than 50,000. For this reason, resilience concept was introduced to consider the power system behavior against natural events. Power distribution system (PDS), on the other hand, is the most vulnerable part of the power system infrastructure, because of its inherent density. For instance, about 90 percent of US power outages are in the distribution system [2]. For this reason, enhancing the resilience of this part of the power system has become more important than other parts. In this regard, the researchers, in recent years, have focused on the restoration methods of the loads in the PDS after natural disasters [3]. MGs' benefits in improving the resilience of the distribution system have been broadly considered in the literature.

The MG has the potential to improve the resilience of the power system by supplying local and non-local loads [4]. In [5], it has been assumed that the MGs exist before the event of an incident, and they can increase the system resilience by restoring their local loads as well as restoring other loads during the outage. In these papers, MG formation and also the presence of EVs in the PDS were not studied. Given the fact that the growth of the number of the MGs is slow, because of its high cost, it is expected that the number of the MGs in the future PDS will not be large enough to be effective from resilience perspective. So, several references have investigated the dynamic formation of the MGs in the PDS which does not already have any MG. In [6], authors introduced a novel MG formation approach to restoring the CLs using DERs and proposed a resilient multi-agent coordination scheme distributed through local communications to detect the

overall information of the network. Potential loop paths were not considered in this reference. This problem is solved in [7] by considering the impact of tie-switches in MG formation problem; however, the possibility of using multiple resources in a MG was not taken into consideration. The limitation of the aforementioned work was considered in reference [8]. In this reference, using the master-slave control technique, multiple resources can be used to restore loads in each MG. However, uncertainty of the generation power of renewable energy resources and consumed load is neglected in this study. In addition, integrating the master resources in a MG was not considered in the paper. Motivated by this, reference [9] proposed heuristic approach for MG formation under the deterministic and stochastic framework. This reference presented the post and pre-disturbance models for MG formation problem. Authors in [10], after defining different dimensions of the resilience concept in the PDS, used renewable energy resources in MG formation to restore loads under a two-stage stochastic programming framework. In this paper, fuel-based capability of PHEVs and also EVs presence were not considered. Moreover, the introduced method did not cover the mesh network. Despite many studies on MG formation using DERs, less attention has been paid to employing the EVs in MG formation approach and this area is a gap in recent studies.

In recent years, EVs have been considered as an inevitable solution to reduce air pollution and reduce fossil fuel consumption. Penetration of the EVs has been increased and result in having a significant impact on the power system studies [11]. The aggregation of the EVs with V2G and G2V capabilities enables them to participate in ancillary services, such as frequency control, voltage control, and demand response program. Also, the PDS operator can utilize these flexible resources to enhance PDS resilience. In [12], a hybrid approach was considered to use DERs to increase the resilience of the PDS. In the proposed model, the combined use of the PHEVs and PV systems was considered in a smart house. The PDS was not considered and the integration of PV and a PHEV only studied in a smart house. The possibility of using battery electric vehicles (BEVs) and PHEVs to supply residential loads in a smart house during the power outages was investigated in [13]. In this paper, also the PDS and MG formation were not considered. In [14], the electrical energy of the PHEVs, as well as the fossil fuel energy stored in fuel tank, were considered to supply residential loads. Authors in [15] developed a two-stage optimization model for employing EVs in MG restoration after natural disasters. In this paper, the island and grid-connected operation of only one MG is considered. The study reported in [4] examined the resilience enhancement of the PDS using hybrid MGs and employing EVs. Some key features such as considering mesh networks and deploying control strategies for DGs were not considered in this paper.

All studies done in the mentioned papers limited to a smart house and MG formation and PDS were not considered. To be noted that none of these studies has addressed the use of BEVs and PHEVs, parked in public or residential parking lots, in the form of restoring CLs in a power distribution system. Enhancing the resilience of the PDS by using electrical and chemical energy of the EVs, as the one of the features that are possible using V2G and G2V capabilities, was not mentioned in any of the previous studies.

Table I: Comparison of this study to other references

Framework			Deterministic										Stochastic				
References			[1]	[3]	[4]	[5]	[6]	[7]	[8]	[12]	[13]	[14]	[3]	[9]	[15]	[10]	This paper
Features	Considering MG formation		-	-	-	-	✓	✓	✓	-	-	-	-	✓	-	✓	✓
	Considering radial network		✓	✓	✓	✓	✓	✓	✓	-	-	-	✓	✓	✓	✓	✓
	Considering mesh network		-	-	-	-	-	✓	✓	-	-	-	-	✓	-	✓	✓
	Master-slave control		-	-	-	-	-	-	✓	-	-	-	-	-	-	✓	✓
	Demand response		✓	✓	✓	✓	-	-	-	-	-	-	✓	✓	✓	✓	✓
	Using EVs	Using the electrical energy of EVs	-	-	✓	-	-	-	-	✓	✓	✓	-	-	✓	-	✓
		Using the fuel-based capability of PHEVs	-	-	-	-	-	-	-	-	✓	✓	-	-	-	-	✓

In the present study, we intend to use the electrical and chemical energy stored in the BEVs and PHEVs, along with the participation of distributed generations (DG) and PVs in the MGs formation to restore CLs after natural disasters. A novel method for restoring CLs in mesh network is presented. Also, a two-stage stochastic framework is proposed for modeling the MG formation problem due to uncertainties in the parameters of EVs, PVs, and hourly load consumption. A comparison of suggested approaches employed in this paper to other references are shown in Table 1. As presented in Table 1, this study, taking into account the shortcomings of recent works and trying to provide a comprehensive model of MG formation. This paper attempts to address the four main shortcomings identified in the recent works as below:

1) In reference [6], only the radial network is considered. Therefore, this paper proposes a new method for restoring loads in the mesh network.

2) Using multiple sources in a MG is not considered in [7]. In this paper, using the Master-slave technique, it is possible to use several resources in one MG.

3) The ability to control the load and consequently the optimal use of energy resources has not been seen in references [6]-[8]. To overcome this limitation, load control blocks are fully modeled in this paper.

4) EVs and PHEVs and their stochastic nature are not considered in recent studies in resilience. This paper proposes a two-stage stochastic approach to model the BEVs and PHEVs in MG formation problem.

Considering the EVs in the resilience studies pose challenges, such as regulatory policies, social and economic impacts, and technology-related restrictions. The details of these challenges and the solutions to each are beyond the scope of this paper and authors assume that distribution system operator (DSO) has enough capability to persuade EVs for cooperation in the program. This paper provide a comprehensive method to integrate flexible resources such as EVs and EGs embedded in PHEVs in MGs formation problem beside other available resources such as demand response program and DGs. In order to model the uncertainties of the EVs' parameters, and to consider all possible scenarios for these resources, modeling has been done based on a two-stage stochastic framework.

The main contributions/novelties of this paper can be summarized as follows:

- A novel method is proposed for modelling load restoration in a power distribution system based on a two-stage stochastic programming framework considering load control capabilities.
- A novel mathematical model is proposed to critical loads restoration in a mesh network, and employing plug-in hybrid electric vehicles as distributed energy resources in a linear framework.
- Both electric vehicles and plug-in hybrid electric vehicles are considered as available energy resources for the formation of MGs.

The remainder of this paper is organized as follows: In section 2, the integration of BEVs and PHEVs and energy management of them before the event is discussed. MG formation constraints and its objective function are formulated in section 3. Simulation results are presented in Section 4. Finally, in Section 5, concluding remarks are made.

2. Integration of Battery Electric Vehicles and Plug-in Hybrid Electric Vehicles

As mentioned before, EVs can play an important role in enhancing the PDS resilience by taking part in their stored energy to restore CLs after the natural disaster. It is assumed that EVs' owner behaviors are the same as before, so two issues need to be considered about the EVs before modeling the problem. 1) The charge/discharge scheduling of the EVs before the event must be considered to determine the condition of the EVs battery for participating in MG formation; 2) Fuel consumption and power generation modeling of the PHEVs should be considered to specify operating conditions of their EGs during the outage. For this reason, we first discuss the charge/discharge scheduling of the EVs in Section 2.1, then, in section 2.2, a linear power generation model for EGs embedded in PHEVs is presented.

It should be noted that due to the unclear traffic flow situation on the roads after the incident, in this study, the study of traffic management in solving the problem is avoided.

2.1 Charge/discharge scheduling of the Electric Vehicles before natural disaster

In general, any EV on the power system is shown as a "noise". Therefore, in order to provide any service to the power system, EVs should be organized by an aggregator [16]. Each aggregator also has the task of charge/discharge scheduling of the EVs. In this study, charging /discharging of the EVs in normal condition is formulated as the following MILP problem [17]:

$$Min: ObjF = \sum_{t=tarr}^{tdep} \Delta t\left(P_{ch_e}^t C^t - P_{dch_e}^t R^t\right) \quad (1)$$

$$0 \le P_{ch_e}^t \le P_{ch}^{max}.\, n_{ch_e}^t \qquad \forall t \in T \quad (2)$$

$$0 \le P_{dch_e}^t \le P_{dch}^{max}.\, n_{dch_e}^t \qquad \forall t \in T \quad (3)$$

$$SOC^{min} \le SOC_e^t \le SOC^{max} \qquad \forall t \in T \quad (4)$$

$$SOC_e^{t+1} = SOC_e^t + \left(n_{ch_e}^t P_{ch_e}^t \eta^{ch} - \frac{n_{dch_e}^t P_{dch_e}^t}{\eta^{dch}}\right)\Delta t \qquad \forall t \in T \quad (5)$$

$$n_{ch_e}^t + n_{dch_e}^t \le 1 \qquad \forall t \in T \quad (6)$$

$$SOC_e^{t_{arr}} = SOC^{initial} \quad (7)$$

$$SOC_e^{t_{dep}} = SOC^{final} \quad (8)$$

According to (1), the total cost for each EV, which consists of the charging cost term and discharging reward term, should be minimized during the EV parking duration. In this equation C^t and R^t, respectively, are the charging cost and reward payment of the EVs at the time t. Constraints (2) and (3), respectively, indicate the charge and discharge limit of the EVs according to the status of their charge and discharge control variables. Constraint (4) guarantees that the SOC of any EV is always within its permissible range. The SOC of each EV is determined by using the constraint (5). Constraint (6) guarantees that for each EV, no simultaneous charging and discharging is possible per hour. Constraints (7) and (8), imply that the SOC of the EV at the arriving time must be equal to its initial SOC and the SOC of the EV at the departure time must be equal to its final expected SOC. Charge/discharge scheduling of the EVs during the outage duration will be discussed in Section 3.4.5.

2.2 Modeling of the Engine Generator

Due to the increased internal power consumption of the current PHEVs and, to help the battery in the journey of more than 350 miles, an onboard EG is embedded in PHEVs [18]. The large fuel tank of the EG allows us to use this power resource along with PHEV's battery for loads restoration in emergencies [14]. To model the EG of the PHEV, we first need to consider the system that converts the chemical energy stored in a gasoline tank into electrical energy. The concept of brake specific fuel consumption (BSFC) is typically used to measure the ratio of fuel consumption to power output, the unit of which is (g/kWh). Generally, at a given operating point with specified speed and torque of the generator, a certain amount of electrical power will be generated by the engine-generator.

If the BSFC parameter is specified at this point of operation, the amount of fuel consumed at that point can be calculated. This is the amount of fuel consumed per minute in EG. A quadratic equation is obtained by fitting the curve to the data measured by the sample EG [14]. For example, the relationship between fuel consumption and power output of the "Chevrolet Volt" is shown in equation (9). In this equation, *g(t)* is the consumed fuel in hour *t*, and *P(g(t))* is the amount of power generated in the EG at that hour. It should be noted that in this equation, the time scale is one hour. The energy conversion curve obtained from equation (9) is shown in Fig. 1. The linearization of such equations in optimization problems is proposed in [19].

$$P\big(g(t)\big) = -0.000105 \times g(t)^2 + 5.291 \times g(t) + 588.3 \qquad (9)$$

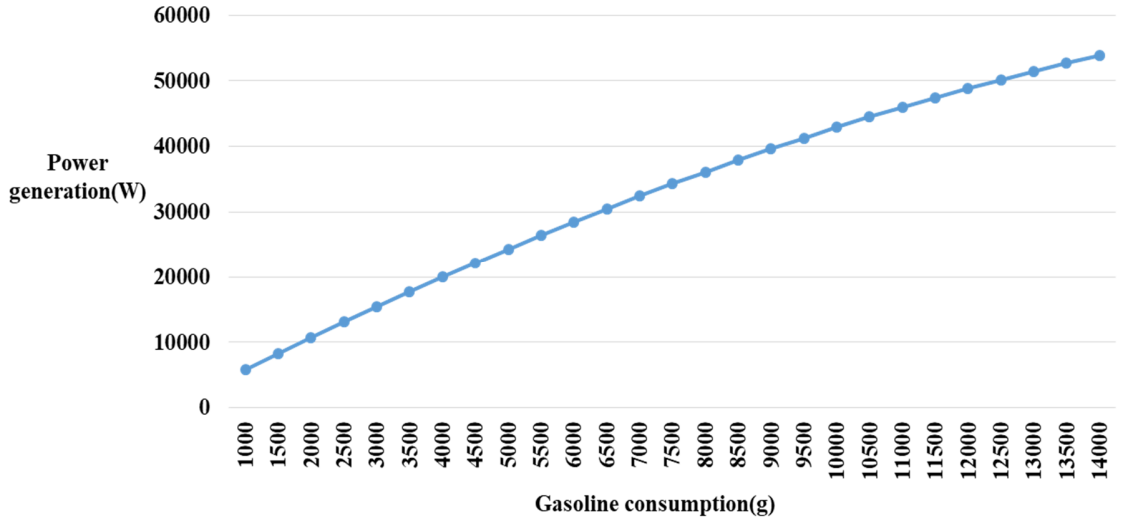

Fig. 1. Constant power generation during 1 hour with Gasoline consumption for “Chevrolet Volt” EG model.

3. Micro-Grid formation problem

In this section, the dynamic formation of MGs to restore the CLs by considering the EVs and load control employment is modeled. The proposed approach integrates the topological and electrical characteristics of the PDS into a linear optimization problem. In addition, this problem is modeled in the two-stage stochastic programming framework, so that the electrical constraints, such as power flow and energy management constraints are divided into two categories: scheduling constraints and operating constraints. This type of uncertainty modeling will be described in Section 3.1. Fig. 2 shows the MGS formation methods and its improved parts.

Methods	Major considerations		
Operation methods	MGs formation in radial networks	+	**MGs formation in mesh networks**
	Considering the uncontrollable loads	+	**Considering the load control capabilities**
	Load restoration using DGs, PVs	+	**Load restoration using EVs and EGs embedded in PHEV**
Type of scheduling	Employing deterministic methods	+	**Employing two stage stochastic method**
Energy resources	Considering one DER in each MG	+	**Considering multiple DERs in each MG**

Fig. 2. MGs formation methods and major considerations.

Several assumptions are considered in modeling the problem, which is outlined below:

- The number of remote control switches is limited in PDS.
- After the incident, in addition to disconnecting from the main grid, some distribution lines and remote control switches may be damaged.
- It is assumed that the system operator is capable of controlling the charging / discharging of the EVs.
- In addition to CLs, some residential loads, which are in the common bus with RPs or PV units, will also be restored.
- Smart meters allow for disconnect the non-critical loads prior to the restoration.
- It is assumed that the PHEVs, which parked just in RPs, can use their EGs to restore CLs.

3.1 Stochastic modeling of the Micro-Grid formation problem

The renewable energy resources and EVs participation in the CLs restoration problem requires proper modeling of uncertainties in the parameters of these resources. Linear two-stage stochastic framework can provide a useful tool for modeling uncertainties in such problems [15]. To model the MG formation problem under the proposed scenario-based framework, we first need to generate a set of scenarios for each of the uncertain parameters. In this regard, by extracting the probability distribution functions (PDFs) of EVs parameters, such as car type, arrival time, departure time and the initial state of charge (SOC), and performing the Monte Carlo simulation (MCS), we obtain the initial set of scenarios for each uncertain parameters. It should be noted that the prediction error of the hourly output power of the PVs and the hourly load consumption, always

follows a normal PDF [17, 21]. Therefore, with the predicted information of these parameters, a set of scenarios can be generated for each of them [22]. Due to increasing the computation burden, after generating the initial set of scenarios, they must be reduced to a smaller set by applying an appropriate scenario reduction method. In this paper, "*forward selection*" method used to reduce the scenarios [15]. After reducing the initial sets of scenarios to the tractable sets, these sets of scenarios for all the parameters are integrated using the scenario integration process, which presented in [22] to create a single set of scenarios for the MG formation problem.

In the proposed linear two-stage framework, two time stages are considered. In the first stage, called the scheduling stage, the scheduled amount of some variables, such as the topological variables (such as status of the remote control switches) and the electrical variables (such as active power generation of energy resources), are taken into account. In the second stage, which is called the operating stage, according to the realization of each scenario, the real-time value of the electrical variables, such as active/reactive power injected to the buses, are considered. In addition, problem constraints are also divided into two groups: scheduling constraints and operating constraints, and at each stage, the relevant constraints are considered. Fig. 3 shows the flowchart of the supplied load calculation in the MG formation problem, which is solved in a linear two-stage stochastic programming framework.

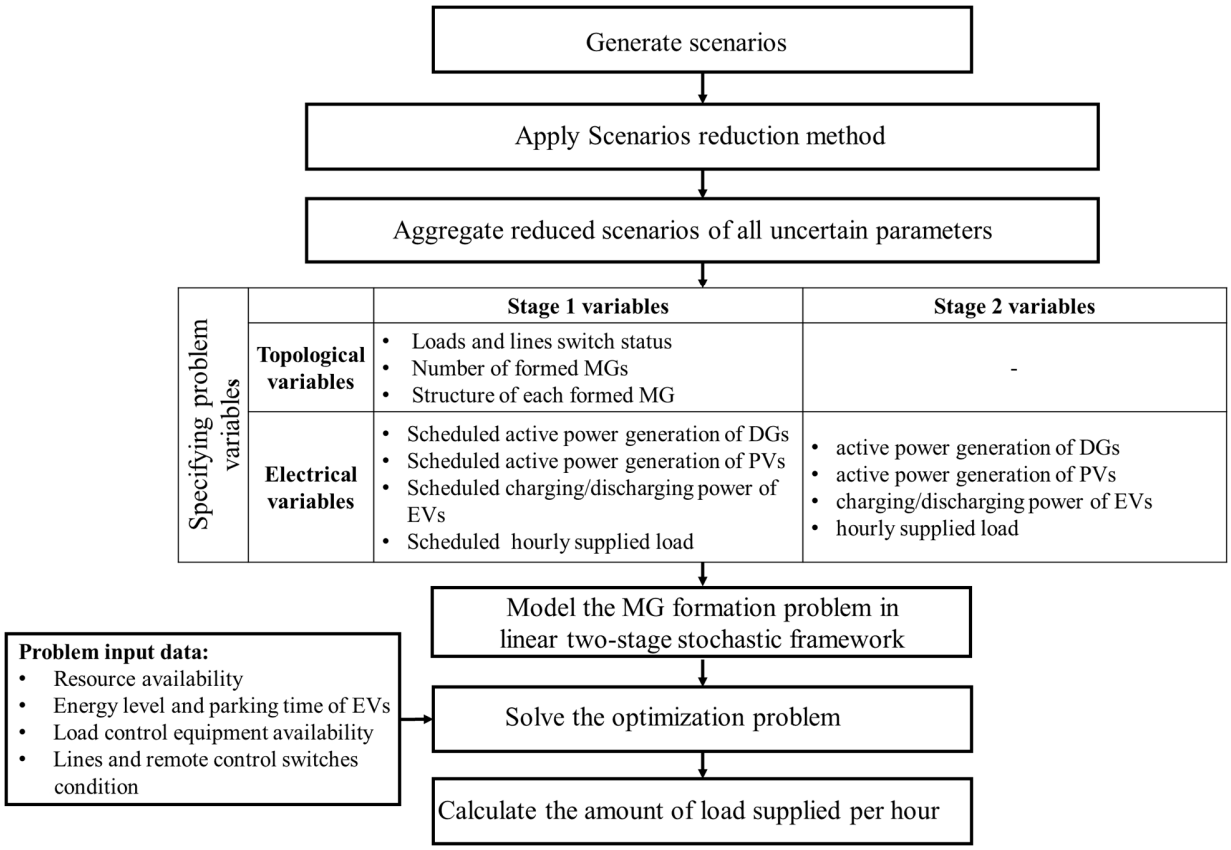

Fig. 3. Flowchart of the supplied load calculation procedure in the MG formation problem

3.2. Topological constraints

In this section, a graph-based theoretical framework for representation of the distribution feeders is presented. In this framework, the distribution network is presented as a graph, "*Dis_graph (N,B)"*, with *N* nodes and *B* branches, where each node represents the bus in the network and each branch represents the distribution feeder. Generally, in this study, MGs are formed under the radial structure to restore CLs. Due to the presence of tie-switches, it is possible to form loops in the PDS. In this condition, there are several possible paths to form the radial MG. If the PDS does not have any tie switches, there will be only one possible path for restoring each CL by the master resource. In this study, MG formation modeling is performed for the radial and mesh parts of the network [7]. Therefore, the topological constraints of the network are divided into three categories: general connectivity constraints, radial part connectivity constraints, and mesh part connectivity constraints.

The four important variables used in these constraints are:

1) $\boldsymbol{\alpha_i^m}$, is the binary variable for all nodes of the network and represents the restoration status of node *i* by the master unit *m*, so if this variable is equal to one, it means that node *i* is restored by the master unit *m*, and vice versa.

2) $\boldsymbol{\beta_{i,\alpha}^m}$, is a binary variable and is defined for all network nodes that have the potential to be in the loop, and represents the restoration status of node *i* by the master unit *m*, through the path α. If this variable is equal to one, it means that node *i* is restored by the master unit *m* and through the path α, and vice versa.

3) $\boldsymbol{l_i}$, which is a binary variable and is defined for all the nodes in the network on which the CL is located, and represents the restoration status of node *i*. If this variable equals one, it means that the load located at node *i* is restored and vice versa.

4) $\boldsymbol{s_i}$, which is a binary variable and is defined for all the nodes in the network on which the slave unit is located, indicating the participation status of node *i*. If this variable is equal to one, it means that the slave unit located at node *i* participates in network restoration and vice versa.

3.2.1 General connectivity constraints

These constraints imply that, with the use of the master-slave control technique, each formed MG has only one master unit with several slave units and CLs. In master-slave control technique, the master unit (such as DGs) controls the voltage and frequency of the MG, and in this voltage and frequency the slave unit which considered as a current controlled source generates active and reactive power. How to apply this technique to the MG formation problem is as follows. In modeling the MG formation problem, the active and reactive power output of the slave units is considered as an independent variable. As a result, the output power of each master unit is calculated from the sum of the load consumed in the formed MG minus the generating power of the slave units in that MG. More information on the master-slave control technique can be found in [23].

Constraint (10) guarantees that node *i* to which the master unit is connected must be restored by that unit. Constraint (11) guarantees that node *i* that is not connected to the critical load must be restored at most by one master unit. Constraint (12) guarantees that node *i* to which the critical

load is connected, depending on the status of its switch (l_i), must be restored by a master unit. Constraint (13) guarantees that node i to which the slave unit is connected can participate in restoration depends on the status of its switch (s_i). Constraint (14) implies that if the line between two nodes i and j is damaged, these two nodes cannot be inside the same MG. Constraint (15) implies that, if the switch between two nodes i and j is damaged, the restoration status of these two nodes must be the same.

$$\alpha_i^m = 1 \qquad \forall i = m\,, m \in N_{\text{master}} \qquad (10)$$

$$\sum\nolimits_{m \in M_{\text{master}}} \alpha_i^m \le 1 \qquad \forall i \notin N_{\text{critical\_load}} \qquad (11)$$

$$\sum\nolimits_{m \in M_{\text{master}}} \alpha_i^m = l_i \qquad \forall i \in N_{\text{critical\_load}} \qquad (12)$$

$$\sum\nolimits_{m \in M_{\text{master}}} \alpha_i^m = s_i \qquad \forall i \in N_{slave} \qquad (13)$$

$$\alpha_i^m + \alpha_j^m \le 1 \qquad \forall i \in \text{N}\,, j \in N_{\text{m,children}}^i\,, m \in N_{\text{master}} \qquad (14)$$

$$\alpha_i^m - \alpha_j^m \le 0 \qquad \forall i \in \text{N}\,, j \in N_{m,\text{children}}^i\,, m \in N_{\text{master}} \qquad (15)$$

3.2.2 Connectivity constraints in radial parts

Constraint (16) guarantees that node i, which does not belong to any potential loop and its parent node must be restored by the same master unit.

$$\alpha_j^m - \alpha_i^m \le 0 \qquad \forall i \in \text{N}, j \in N_{m,\text{children}}^i\,, (\text{i},\text{j}) \notin N_{\text{loop}}, m \in N_{\text{master}} \qquad (16)$$

3.2.3 Connectivity constraints in loop parts

These constraints are defined for the network nodes, which are in the potential loop. As illustrated in Fig. 4, nodes in the potential loop can be restored along different paths. Constraint (17) guarantees that the nodes inside the potential loop can only be restored through one path. It should be noted that the nodes, which are in the potential loop and on which the master unit is located (such as node $\{c\}$ in Fig. 4) and also nodes, which located at the junction of the radial and loop parts and restored earlier by a resource outside the loop (such as node {e, a} in Fig. 4), are not considered in constraint (17). For these nodes, multiple restoration paths are meaningless, and these nodes are restored only from one path; constraint (18) is used to guarantee this fact. Constraint (18) implies that the restoration status of mentioned nodes (status of $\beta_{i,\alpha}^m$) depends on their adjacent nodes. For example, in Fig. 4, the restoration status of the node $\{e\}$ by resource #2 through path #1 ($\beta_{e,1}^2$) depends on the status of the $\beta_{d,1}^2$.

$$\alpha_i^m = \sum\nolimits_{\alpha \in \aleph_{m,i}^{\alpha}} \beta_{i,\theta}^m \qquad \forall i \in N_{\text{loop}}\,, i \notin N_{\text{loop\_DER}}, m \in N_{\text{master}} \qquad (17)$$

$$\beta_{i,\alpha}^m = \beta_{j,\alpha}^m \qquad \forall i \in N_{\text{loop\_DER}},\ \alpha \in \aleph_{k,i}^{\alpha}, j \in N_{m,children}^{i,\alpha}, m \in N_{\text{master}} \qquad (18)$$

Constraint (19) guarantees that, if node i is in a loop restored by master unit m through path α, the variable α_i^m for all nodes in path α, from node i to resource m, must be set to one. When using this constraint in the problem, the "*Yen's k-shortest path*" algorithm is applied to find the shortest possible path between two nodes in the loop [24].

$$\beta_{i,\alpha}^{m} \leq \sum_{j \in N_{m,parent}^{i,\alpha}} \frac{\alpha_j^m}{\left|N_{m,parent}^{i,\alpha}\right|} \qquad \forall (i,j) \in N_{\text{loop}}, \alpha \in \aleph_{m,i}^{\alpha}, m \in N_{\text{master}} \qquad (19)$$

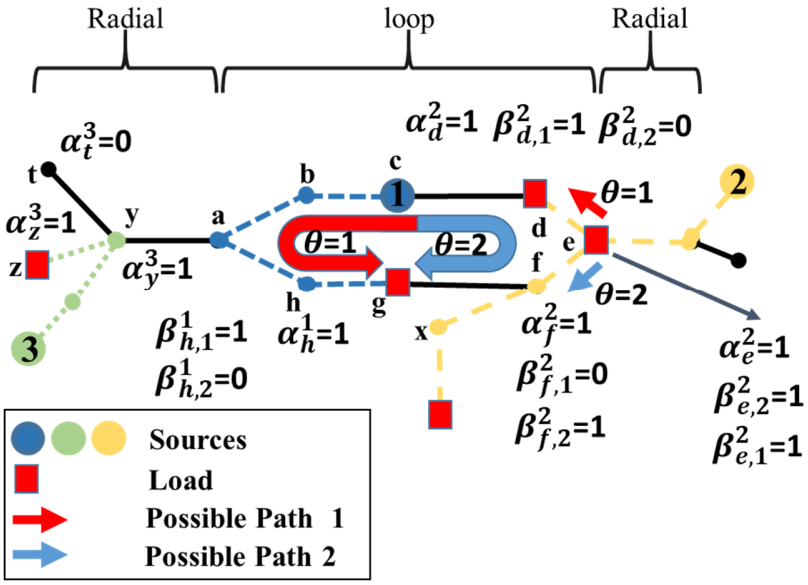

Fig. 4. Illustrative example for various nodes restoration

3.3 Power flow constraints

For each formed MG, the amount of the active and reactive power flowing in the lines, as well as the amplitude of the bus voltage, must be determined. This simplified power flow model named "DistFlow" is used in this study [25]. The reason for using simplified "Distflow" is that the power flow in the lines is relatively low, and therefore, network losses can be neglected [25]. In this study, it is assumed that the active load control is applied in a discrete mode (five steps) by utilizing demand response contracts, small solar panels, etc. In each step, a certain percentage of the supplied load is reduced [10]. In addition, as previously mentioned, for full load interruption, the switch associated with that load, specified by the binary variable (l_i), must be opened. Reactive load control is also modeled according to the load power factor. In the problem modeling, the nonlinear terms generated by multiplying the binary variable into the continuous variable are linearized by the "*BIG M*" method [26].

3.3.1 Power flow constraints in the scheduling stage

In this stage, the scheduled amounts of the active power generated by the various resources in each MG should be equal to the amount of scheduled amount of the loads. This power includes active power generation of the DGs, active power generation of the PV units, EVs' battery charging and discharging powers, and the EGs power generation inside the PHEVs, which are all dependent on the restoration or participation status of their associated nodes. Equation (20) shows this equilibrium. In (21) also, the load control equation is indicated. When control step l is activated at hour t, the associated variable ($\rho_{l,i}^{s,t}$) is set to one, and $P_{control,i}^{s,t,l}$ shows the amount of load reduction from the expected load in the bus i at hour t.

$$[P_{DG,m}^{s,t} + \sum_{i\in PV_{Node}} \alpha_i^m P_{PV,i}^{s,t} + \sum_{i\in EVP_{Node}} \alpha_i^m P_{EVP,i}^{s,dch,t} - \sum_{i\in EVP_{Node}} \alpha_i^m P_{EVP,i}^{s,ch,t} +$$

$$\sum_{i\in EVP_{Node}} \alpha_i^m P_{PHEV,i}^{s,dch,t} = \sum_{i\in CL_{Node}} \alpha_i^m P_{SUP,i}^{s,t}\ ] \qquad \forall m \in N_{master}, t \in T \qquad (20)$$

$$P_{Sup,i}^{s,t} = \overline{P_{critical,i}^{s,t}} - \sum_{l\in L} \rho_{l.i}^{s,t} \times P_{control,i}^{s,t,l} \qquad \forall i \in N, t \in T \qquad (21)$$

3.3.2 Power flow constraints in operating stage

The power flow equations are different in radial and loop parts. In this section, each of these two types of power flows constraints are formulated.

- **Power flow constraints in the radial part**

Constraints (22) and (23) imply that at node *i,* located in the radial part, and in each scenario, the active/reactive power injected to node equals to the sum of the power injected to its children nodes, and the power of supplied load, which located on node *i*. Also, if the slave unit is located on the node *i*, the generation power of the slave unit will decrease from the total power injected into the node *i*.

$$p_i^{m,\omega,t} = \sum_{j\in N_{m,children}^i} p_j^{m,\omega,t} + \alpha_i^m \times (P_{SUP,i}^{\omega,t} - P_{PV,i}^{\omega,t} - P_{EVP,i}^{\omega,dch,t} + P_{EVP,i}^{\omega,ch,t} - P_{PHEV,i}^{\omega,dch,t})$$

$$\forall i \in N, m \in N_{master}, t \in T, \omega \in \Omega \qquad (22)$$

$$q_i^{m,\omega,t} = \sum_{j\in N_{m,children}^i} q_j^{m,\omega,t} + \alpha_i^m \times (Q_{SUP,i}^{\omega,t} - Q_{PV,i}^{\omega,t} - Q_{EVP,i}^{\omega,dch,t} + Q_{EVP,i}^{\omega,ch,t} - Q_{PHEV,i}^{\omega,dch,t})$$

$$\forall i \in N, m \in N_{master}, t \in T, \omega \in \Omega \qquad (23)$$

Constraints (24) illustrates the relationship between the voltage of the nodes *i* and *j* and the active / reactive power injected to the node *j*.

$$V_i^{m,\omega,t} - V_j^{m,\omega,t} = \frac{(r_{ij} p_j^{m,\omega,t} + x_{ij} q_j^{m,\omega,t})}{V_0^k}$$

$$\forall i \in N, \forall j \in N_{m,children}^i, m \in N_{master}, t \in T, \omega \in \Omega \qquad (24)$$

- **Power flow constraints in the loop part**

Constraints (25) and (26) imply that at node *i,* located in the radial part, and in each scenario, the active/reactive power injected to the node along path α equals to the sum of the power injected to its children nodes along the same path and common children node, and the power of supplied load, which located on node *i*. Moreover, if the slave unit is located at node *i*, generation of the slave unit will decrease from the total power injected into the node. The common children nodes of node *i*, which are denoted by set $N_{m,common}^i$, refer to the nodes that are always considered as the children nodes of node *i*, regardless of the restoration path of node *i*. For example, in Fig. 4, node $\{a\}$ is children of node $\{b\}$ along the path 1 and node $\{x\}$ is the common children of node $\{f\}$. Constraint (27) specified the voltage of the node *i* along path α according to the injected active/reactive power into this node along the same path.

$$[p_{i,\alpha}^{m,\omega,t} = p_{j,\alpha}^{m,\omega,t} \times \beta_{j,\alpha}^{m} + \alpha_i^m \times (P_{SUP,i}^{\omega,t} - P_{PV,i}^{\omega,t} - P_{EVP,i}^{\omega,dch,t} + P_{EVP,i}^{\omega,ch,t} - P_{PHEV,i}^{\omega,dch,t}) + \left(\sum_{y \in N_{m,common}^{i}} p_y^{m,\omega,t}\right)]$$

$$\forall i \in N_{\text{loop}}, \alpha \in \aleph_{m,i}, j \in N_{m,children}^{i,\alpha}, m \in N_{\text{master}}, t \in T, \omega \in \Omega \quad (25)$$

$$[q_{i,\alpha}^{m,\omega,t} = q_{j,\alpha}^{m,\omega,t} \times \beta_{j,\alpha}^{m} + \alpha_i^m \times (Q_{SUP,i}^{\omega,t} - Q_{PV,i}^{\omega,t} - Q_{EVP,i}^{\omega,dch,t} + Q_{EVP,i}^{\omega,ch,t} - Q_{PHEV,i}^{\omega,dch,t}) + \left(\sum_{y \in N_{k,common}^{i}} q_y^{k,\omega,t}\right)]$$

$$\forall i \in N_{\text{loop}}, \alpha \in \aleph_{m,i}, j \in N_{m,children}^{i,\alpha}, m \in N_{\text{master}}, t \in T, \omega \in \Omega \quad (26)$$

$$V_{i,\alpha}^{m,\omega,t} - V_{j,\alpha}^{m,\omega,t} = \frac{\left(r_{ij} p_{j,\alpha}^{m,\omega,t} + x_{ij} q_{j,\alpha}^{m,\omega,t}\right)}{V_0^m}$$

$$\forall (\text{i,j}) \in N_{\text{loop}}, j \in N_{m,children}^{i,\alpha}, \alpha \in \aleph_{m,i}, m \in N_{\text{master}}, t \in T, \omega \in \Omega \quad (27)$$

Constraints (28) to (30) are defined to obtain the amount of active/reactive power injected into the nodes, which are located in the potential loop, and also calculate the nodes' voltage after the power flow calculation in different paths. In these constraints, variables $\tau_i^{m,\omega,p}$ and $\tau_i^{m,\omega,q}$, prevent repeating the calculations of the power which is common among all possible paths, such as supplied load, generating power of the slave units and the power injected to the common children nodes. For example, in Fig. 4, the load consumption of node $\{e\}$ is calculated, both through path #1 and through path #2 according to constraint (25). Since both paths have been selected to restore this node, if we do not use the variable $\tau_i^{m,\omega,p}$ in constraint (28), the power consumption of load is calculated two times. As it is clear from equations (31) and (32), variables $\tau_i^{m,\omega,p}$ and $\tau_i^{m,\omega,q}$ can take different values depending on the number of the restored paths in which node *i* is located.

$$p_i^{m,\omega,t} = \left(\sum_{\alpha \in \aleph_{m,i}^{\alpha}} \beta_{i,\alpha}^{m} \times p_{i,\alpha}^{m,\omega,t}\right) - \tau_i^{m,p,\omega,t} \quad \forall i \in N_{\text{loop}}, m \in N_{\text{master}}, t \in T, \omega \in \Omega \quad (28)$$

$$q_i^{m,\omega,t} = \left(\sum_{\alpha \in \aleph_{m,i}^{\alpha}} \beta_{i,\alpha}^{m} \times q_{i,\alpha}^{m,\omega,t}\right) - \tau_i^{m,q,\omega,t}$$

$$\forall i \in N_{\text{loop}}, k \in N_{\text{master}}, t \in T, \omega \in \Omega \quad (29)$$

$$V_i^{m,\omega,t} = \left(\sum_{\alpha \in \aleph_{m,i}^{\alpha}} \beta_{i,\alpha}^{m} \times V_{i,\alpha}^{m,\omega,t}\right)$$

$$\forall i \in N_{\text{loop}}, \forall i \notin N_{\text{loop\_DER}}, \text{m} \in N_{\text{master}}, t \in T, \omega \in \Omega \quad (30)$$

$$\tau_i^{m,p,\omega,t} = \left(\left(\sum_{\alpha \in \aleph_{m,i}^{\alpha}} \beta_{i,\alpha}^{m}\right) - 1\right) \times \left(\begin{array}{c} \left(\sum_{y \in N_{m,common}^{i}} p_y^{m,\omega,t}\right) + \\ \alpha_i^m \times (P_{SUP,i}^{\omega,t} - P_{PV,i}^{\omega,t} - P_{EVP,i}^{\omega,dch,t} + P_{EVP,i}^{\omega,ch,t} - P_{PHEV,i}^{\omega,dch,t}) \end{array}\right)$$

$$\forall i \in N_{\text{loop}}, m \in N_{\text{master}}, t \in T, \omega \in \Omega \quad (31)$$

$$\tau_i^{m,q,\omega,t} = \left(\left(\sum_{\alpha\in\aleph_{m,i}^{\alpha}} \beta_{i,\alpha}^{m}\right) - 1\right) \times \left(\begin{array}{c} \left(\sum_{y\in N_{m,common}^{i}} q_y^{m,\omega,t}\right) + \\ \alpha_i^m \times (Q_{SUP,i}^{\omega,t} - Q_{PV,i}^{\omega,t} - Q_{EVP,i}^{\omega,dch,t} + Q_{EVP,i}^{\omega,ch,t} - Q_{PHEV,i}^{\omega,dch,t}) \end{array} \right)$$

$$\forall i \in N_{\text{loop}}, m \in N_{\text{master}}, t \in T, \omega \in \Omega \quad (32)$$

Constraints (33) and (34) model the load control at node *i* in each scenario.

$$P_{Sup,i}^{\omega,t} = P_{critical,i}^{\omega,t} - \sum_{l\in L} \rho_{l.i}^{\omega,t} \times P_{control,i}^{\omega,t,l} \qquad \forall i \in N, t \in T, \omega \in \Omega \quad (33)$$

$$Q_{Sup,i}^{\omega,t} = Q_{critical,i}^{\omega,t} - \sum_{l\in L} \rho_{l.i}^{\omega,t} \times P_{control,i}^{\omega,t,l} \times \tan(\varphi_i) \qquad \forall i \in N, t \in T, \omega \in \Omega \quad (34)$$

3.4 Network and resource constraints

This set of constraints is used to guarantee that the network's variables, power resources' variables, and the amount of the usable load control blocks are in the permissible ranges. Constraint (35) implies that the voltage of the buses can vary between 95% and 105% of the rated voltage. It should be noted that the voltage and reactive power limitations are not considered at the scheduling stage.

$$0.95 \times V_0^m \le V_i^{m,\omega,t} \le 1.05 \times V_0^m \qquad \forall i \in \mathrm{N}, m \in N_{\text{master}}, t \in T, \omega \in \Omega \quad (35)$$

3.4.1 Power and energy limitations of Distributed Generations

Generally, the capacity of DGs, which control the voltage and frequency in MGs as the master units, is limited. Constraints (36) and (37) are used to model the scheduled power generation of the DGs and the amount of fuel consumption, respectively.

$$0 \le P_{DG,m}^{s,t} \le p_m^{max} \qquad \forall m \in N_{master}, t \in T \quad (36)$$

$$\sum_{t=t_{rs}}^{t=t_{re}} P_{DG,m}^{s,t} \le |T| \times CAP^m \qquad \forall m \in N_{master} \quad (37)$$

Constraints (38) to (40) illustrate the limitations on the use of DGs in each scenario, including the limitations of active power, reactive power, and fuel capacity of resources.

$$0 \le p_m^{m,\omega,t} \le p_m^{max} \qquad \forall m \in N_{master}, t \in T, \omega \in \Omega \quad (38)$$

$$0 \le q_m^{m,\omega,t} \le q_m^{max} \qquad \forall m \in N_{master}, t \in T, \omega \in \Omega \quad (39)$$

$$\sum_{t=t_{rs}}^{t=t_{re}} p_m^{m,\omega,t} \le |T| \times CAP^m \qquad \forall m \in N_{master}, \omega \in \Omega \quad (40)$$

3.4.2 Power limitations of Photovoltaic resources

The maximum generation power of the PVs is one of the uncertain parameters determined after the realization of generated scenarios. In the same way, when scheduling the power of these units, the expected maximum output power can be taken into account. The expected maximum output power of the PVs is calculated according to (41), where $P_{PV,i}^{max,\omega,t}$ is the maximum power realized for each scenario and, $P_{PV,i}^{max,s,t}$ is the maximum expected output power of the PVs. Constraint (42) guarantees that the scheduled output power of each PV must be in permissible

range, and the constraints (43) and (44), respectively, show the active and reactive power limitations in the operating stage in each scenario.

$$.P_{PV,i}^{max,s,t} = \sum_{\omega \in \Omega} \pi_{\omega} \times P_{PV,i}^{max,\omega,t} \quad (41)$$

$$0 \leq P_{PV,i}^{s,t} \leq P_{PV,i}^{max,s,t} \quad (42)$$

$$0 \leq P_{PV,i}^{\omega,t} \leq P_{PV,i}^{max,\omega,t} \quad (43)$$

$$0 \leq Q_{PV,i}^{\omega,t} \leq Q_{PV,i}^{max,\omega,t} \quad (44)$$

$$\forall i \in N, t \in T, \omega \in \Omega$$

3.4.3 Scheduling and operating constraints of the Electric Vehicles

After the formation of the MGs, the charge and discharge management of the EVs should also be considered. In this section, as before, there are two types of formulation, scheduling and operating. Constraints (45) to (50) guarantee that the sum of the charge and discharge power of all EVs is equal to the power consumed/injected from/to the bus where the parking lot is located on it. Generally, in the parking lots, reactive power can be controlled using power factor correction tools. Regarding the reactive power consumption or generation of the EVs, it should be noted that there is a general relation between the apparent power of EVs battery and its active or reactive power, which presented in (51) [27]. It is assumed that PLs and distribution substations for residential areas can control reactive power consumption/generation by modifying the power factor of EVs up to a maximum of a certain factor of active power. This factor is shown in constraints (48) and (50) with *S*. The uncertain parameters of each EVs and PHEVs are arrival time, departure time, initial SOC, final desired SOC, initial gasoline and final desired gasoline.

$$P_{EVP,i}^{s,ch,t} = \sum_{e \epsilon M_{EV,i}} n_{e,i}^{s,t,ch} p_{e,i}^{s,t,ch} \quad (45)$$

$$P_{EVP,i}^{s,dch,t} = \sum_{e \epsilon M_{EV,i}} n_{e,i}^{s,t,dch} p_{e,i}^{s,t,dch} \quad (46)$$

$$P_{EVP,i}^{\omega,ch,t} = \sum_{e \epsilon M_{EV,i}} n_{e,i}^{\omega,t,ch} p_{e,i}^{\omega,t,ch} \quad (47)$$

$$Q_{EVP,i}^{\omega,ch,t} \leq S \times \sum_{e \epsilon M_{EV,i}} n_{e,i}^{\omega,t,ch} p_{e,i}^{\omega,t,ch} \quad (48)$$

$$P_{EVP,i}^{\omega,dch,t} = \sum_{e \epsilon M_{EV,i}} n_{e,i}^{\omega,t,dch} p_{e,i}^{\omega,t,dch} \quad (49)$$

$$Q_{EVP,i}^{\omega,dch,t} \leq S \times \sum_{e \epsilon M_{EV,i}} n_{e,i}^{\omega,t,dch} p_{e,i}^{\omega,t,dch} \quad (50)$$

$$Q_{ch/dch}^{max,accessable} = \sqrt{\left(S_{ch/dch}^{max}\right)^2 - \left(P_{ch/dch}^{max}\right)^2} \quad (51)$$

$$\forall i \in N, t \in T, \omega \in \Omega$$

Constraints (52) to (57) guarantee that the charge/discharge power of the EVs as well as the SOC of the batteries do not exceed their expected maximum value in the scheduling stage and their maximum value operating stage.

$$0 \le p_{e,i}^{s,t,ch} \le p_{e,i}^{s,ch,max} \quad (52)$$

$$0 \le p_{e,i}^{s,t,dch} \le p_{e,i}^{s,dch,max} \quad (53)$$

$$0 \le p_{e,i}^{\omega,t,ch} \le p_{e,i}^{\omega,ch,max} \quad (54)$$

$$0 \le p_{e,i}^{\omega,t,dch} \le p_{e,i}^{\omega,dch,max} \quad (55)$$

$$SOC_{e,i}^{s,min} \le SOC_{e,i}^{s,t} \le SOC_{e,i}^{s,max} \quad (56)$$

$$SOC_{e,i}^{\omega,min} \le SOC_{e,i}^{\omega,t} \le SOC_{e,i}^{\omega,max} \quad (57)$$

$$\forall i \in N\ , e \epsilon M_{EV,i}\ , t \in\ T\ , \omega \in\ \Omega$$

3.4.4 Scheduling and operating constraints of the Engine Generators embedded in Plug-in Hybrid Electric Vehicles

In this study also the impact of EGs in PHEVs has been considered. As stated earlier in section 2.2, the relationship between the EG output power and its fuel consumption is nonlinear, so according to [19], this relation must be approximated by a linear piecewise function. Therefore, the nonlinear constraint for each EV in the scheduling stage is transformed into linear constraints (58) to (63). In constraints (62) and (63), respectively, the binary variable $y_{i,e}^{s,t}$ is used to control the EG on and off state, and the parameter $g_{i,e}^{s,fix}$ indicates constant fuel consumption of the EG when it is on.

$$p_{e,i}^{EG,s,t} = \sum_{z \in Z} a_z g_{z,i,e}^{s,t} + b_{e,i} \times g_{i,e}^{s,t} + d_{e,i} \quad (58)$$

$$g_{i,e}^{s,t} = \sum_{z \in Z} a_z g_{z,i,e}^{s,t} \quad (59)$$

$$0 \le g_{z,i,e}^{s,t} \le 3600 \quad (60)$$

$$\forall i \in N, e \epsilon M_{EG,i}, t \in\ T, z \in Z = \{1,2,3\}$$

$$g_{3,i,e}^{s,t} \le g_{2,i,e}^{s,t} \le g_{1,i,e}^{s,t} \quad (61)$$

$$0 \le g_{i,e}^{s,t} \le (g_{i,e}^{s,max} - g_{i,e}^{s,min}) \times y_{i,e}^{s,t} \quad (62)$$

$$\forall i \in N, e \epsilon M_{EG,i}\ , t \in\ T$$

$$\sum_{t \in T} (g_{i,e}^{s,t} + y_{i,e}^{s,t} \times g_{i,e}^{s,fix}) \le \left(FR_{e,i}^{initial} - FR_{e,i}^{min,allowed}\right) \quad (63)$$

$$\forall i \in N, e \epsilon M_{EG,i}$$

Linear Constraints (64) to (69) indicate the limitations of the EGs embedded in the operating stage.

$$p_{e,i}^{EG,\omega,t} = \sum_{z \in Z} a_z g_{z,i,e}^{\omega,t} + 5.291 \times g_{i,e}^{\omega,t} + 588.3 \quad (64)$$

$$g_{i,e}^{\omega,t} = \sum_{z \in Z} a_z g_{z,i,e}^{\omega,t} \quad (65)$$

$$0 \le g_{z,i,e}^{\omega,t} \le 3600 \quad (66)$$

$$\forall i \in N, e \epsilon M_{EG,i}, t \in T, z \in Z = \{1,2,3\}, \omega \in \Omega$$

$$g_{3,i,e}^{\omega,t} \le g_{2,i,e}^{\omega,t} \le g_{1,i,e}^{\omega,t} \quad (67)$$

$$0 \le g_{i,e}^{\omega,t} \le (g_{i,e}^{\omega,max} - g_{i,e}^{\omega,min}) \times y_{i,e}^{\omega,t} \quad (68)$$

$$\forall i \in N, e \epsilon M_{EG,i}, t \in T, \omega \in \Omega$$

$$\sum_{t \in T} (g_{i,e}^{\omega,t} + y_{i,e}^{\omega,t} \times g_{i,e}^{\omega,fix}) \le \left(FR_{e,i}^{initial} - FR_{e,i}^{min,allowed}\right) \quad (69)$$

$$\forall i \in N, e \epsilon M_{EG,i}, \omega \in \Omega$$

3.4.5 Energy management of Electric Vehicles during the outage

The expected value of all the scenarios is used to calculate the initial energy and the desired final energy of the EVs in scheduling stage. The time of arrival and departure of EVs in this stage is also the expected value of all scenarios. Regarding the definition of initial and desired energy constraints, it should be noted that different modes of charging and energy management should be taken into account when considering the time of arrival and departure of the EVs and the outage period. In general, according to Fig. 5, there are six situations for the time of arrival and departure of the EVs according to the outage period. We can manage the charging and discharging of the EVs during the outage period by setting the control variables (such as $n_{e,i}^{s,t,ch}$, $n_{e,i}^{s,t,dch}$, $y_{i,e}^{s,t}$, etc.) as well as determining the amount of EVs' energy at the start of the outage time and the end of the outage period or when the EV exits the parking lot. For example, if we consider the state 2 in Fig. 5, according to equation (70), the energy of the EVs which arrived at the parking lot before the outage occurrence equal to the amount of energy that the aggregator had considered for those EVs at that time (if aggregator was aware of or not aware of the approximate time of the outage). In the case of the EV's energy when it leaves the parking lot, the OMS must act in accordance with the contract concluded with the EV owners. The EV owner announces the minimum amount of final energy that wants after participating in the V2G emergency program to the aggregator, and the aggregator does not allow the OMS to use the energy of the EVs more than the specified amount. Constraint (71) shows this condition for state 2 in Fig. 5. Also, in state 2, according to equations (72) and (73), all battery's charge and discharge control variables and the status variable of the EGs should equal to zero after the EVs departure. Constraints (74) to (77) describe the constraints (70) to (73) in operating stage. In the same way, the energy and power management constraints for all the situations presented in Fig. 5 are obtained, which should be taken into account in the proposed model.

$$SOC_{e,i}^{s,trs} = SOC_{e,i}^{s,initial} \qquad \forall i \in N, e \epsilon M_{EV,i,group2} \quad (70)$$

$$SOC_{e,i}^{s,T_{dep}} \leq SOC_{e,i}^{s,desired} \qquad \forall i \in N\,, e\epsilon M_{EV,i,group2} \qquad (71)$$

$$\sum_{e\epsilon M_{EV,i,group2}} \sum_{t=T_{dep}}^{tre} n_{e,i}^{s,t,ch} + n_{e,i}^{s,t,dch} = 0 \qquad \forall i \in N \qquad (72)$$

$$\sum_{e\epsilon M_{EG,i,group2}} \sum_{t=T_{dep}}^{tre} y_{i,e}^{s,t} = 0 \qquad \forall i \in N \qquad (73)$$

$$SOC_{e,i}^{\omega,trs} = SOC_{e,i}^{\omega,initial} \qquad \forall i \in N\,, e\epsilon M_{EV,i,group2}\,, t \in T\,, \omega \in \Omega \qquad (74)$$

$$SOC_{e,i}^{\omega,t_{dep}} \leq SOC_{e,i}^{\omega,desired} \qquad \forall i \in N\,, e\epsilon M_{EV,i,group2}\,, t \in T\,, \omega \in \Omega \qquad (75)$$

$$\sum_{e\epsilon M_{EV,i,group2}} \sum_{t=t_{dep}}^{tre} n_{e,i}^{\omega,t,ch} + n_{e,i}^{\omega,t,dch} = 0 \qquad \forall i \in N\,, \omega \in \Omega \qquad (76)$$

$$\sum_{e\epsilon M_{EG,i,group2}} \sum_{t=t_{dep}}^{tre} y_{i,e}^{\omega,t} = 0 \qquad \forall i \in N\,, \omega \in \Omega \qquad (77)$$

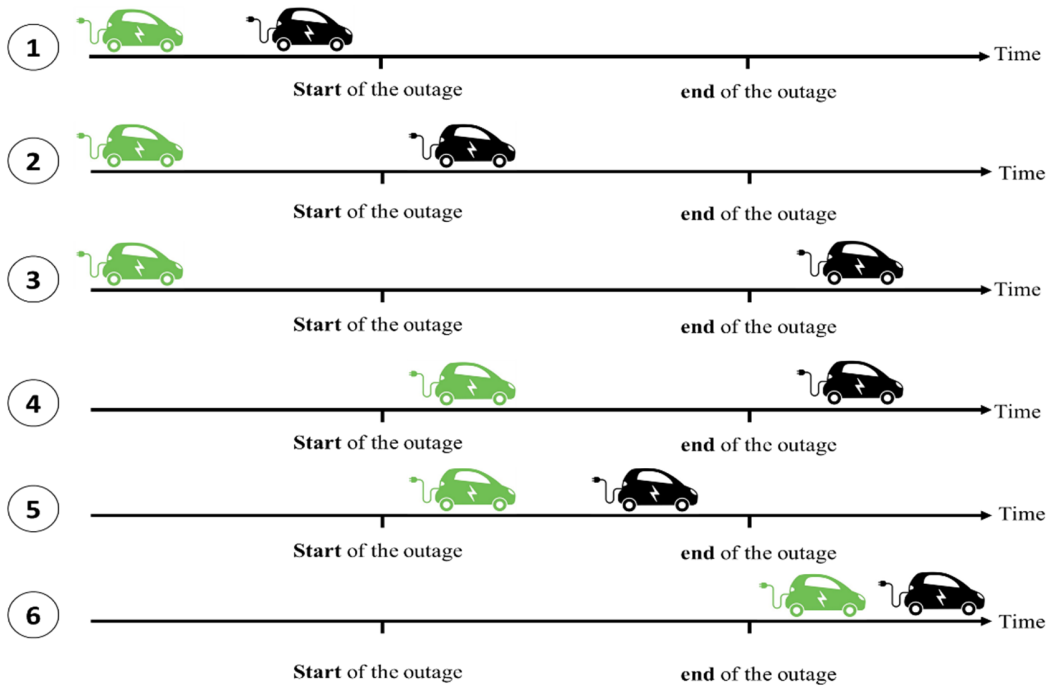

Fig. 5. Different states of arrival / departure of the EVs at / from the parking lot depending on the start of the outage and end of the outage

3.5 Objective function

After presenting the decision variables and constraints of the linear two-stage stochastic programming problem, specifying the objective function of the problem is the final step. In general, in the most power system resilience schemes, the objective function is to approach the point at which the system operated before the outage occurs. For this reason, the objective function in this study is defined as the maximum load restoration and thus the least load control blocks used during restoration. In the two-stage stochastic programming framework, in addition to defining the intended objective function (which should be optimized at the scheduling stage), it must also be

ensured that the impact of all scenarios in decision-making is taken into account according to their probability. So, according to (78), the objective function of the problem consists of two terms, the first term is supplied load in the scheduling stage, and the second term is the distance between the scheduling and expected utilization amount of load control blocks.

$$Min: ObjF = \left(\sum_{t\in T}\sum_{i\in N_{critical_{load}}}(-P_{Sup,i}^{s,t} + \sum_{l\in L}(\rho_{l.i}^{s,t} \times P_{control,i}^{s,t,l} - \sum_{\omega\in\Omega}\pi_{\omega} \times (\rho_{l.i}^{\omega,t} \times P_{control,i}^{\omega,t,l}))\right) \quad (78)$$

To evaluate the performance of the system proposed in different conditions, we have used the resilience index (RI), which is introduced in [10]. Using this metric, the ratio of the scheduled amount of restored loads to the total amount of the loads can be calculated.

$$Resilience\ index = \frac{\sum_{t\in T}\sum_{i\in N_{critical_{load}}} P_{Sup,i}^{s,t}}{\sum_{t\in T}\sum_{i\in N_{critical_{load}}} P_{critical,i}^{s,t}} \quad (79)$$

4. Numerical results

The proposed method is tested on IEEE 123-bus test system (see Fig. 6) and the real 20 kV distribution network located in Sa'adat-Abad district of Tehran, Iran (case study 4). The problem was modeled as a MILP formulation in MATLAB R2015b and solved using CPLEX solver. To use CPLEX solver through MATLAB, IBM ILOG CPLEX 12.6 is linked with MATLAB R2015b. The simulation is executed on a PC with Intel Core i7-6500u @ 2.5 GHz processor and 8 GB of RAM. In order to validate the proposed method, four case studies are designed. In all four cases, it is assumed that after the incident, the upstream network cannot supply the PDS and that some feeders and remote control switches are not available for the restoration, The outage duration is assumed to be 10 hours. The reduced set of scenarios includes 10 scenarios with a probability of 0.1, 0.12, 0.05, 0.08, 0.1, 0.17, 0.13, 0.05, 0.14 and 0.06, respectively. The position of the loads and energy resources in the PDS are shown in Fig. 6. According to [1] and [28], there are 11 CLs in the PDS that their maximum load demand are given in Table II. Fig. 7 shows the load scenarios in each hour. There are four DGs as master units and two PVs as slave units; Tables III and IV depict the specification of DGs and PVs, respectively. Historical information of the PVs power generation has been extracted from [29]. The curves of the PVs generation coefficients for each scenario are also shown in Fig. 8. In the case of EVs, the PDFs of the uncertain parameters are extracted from [30], and the other information of them is shown in Tables V and VI. In general, the number of the EVs at each bus per day (from 6:00 am to 11:59 pm) is assumed to be 15. It should be noted that the loads on the buses containing the RPs and the PV units are also considered in the simulation, and it is also assumed that only PHEVs parked in RPs can use their fossil fuel to restore loads. The factor for reactive power correction (S) is 0.5 in this study.

Table II: load parameters

Load	Bus	Load type	P^{max}(kW)	Q^{max}(kVar)	Load	Bus	Load type	P^{max}(kW)	Q^{max}(kVar)
1	9	Critical	78.6	18.6	9	87	Critical	40.1	66.84
2	17	Critical	29.32	14.34	10	79	Critical	21.84	63.78
3	27	Critical	66.97	36.94	11	101	Critical	50.56	19.87
4	30	Critical	61.2	30.37	12	16	Normal	18.5	8.8
5	37	Critical	18.21	31.6	13	250	Normal	15.5	10.3
6	46	Critical	42.5	27.9	14	12	Normal	19	12.3
7	66	Critical	30.5	25.9	15	81	Normal	14	5.8
8	94	Critical	30.12	21.3					

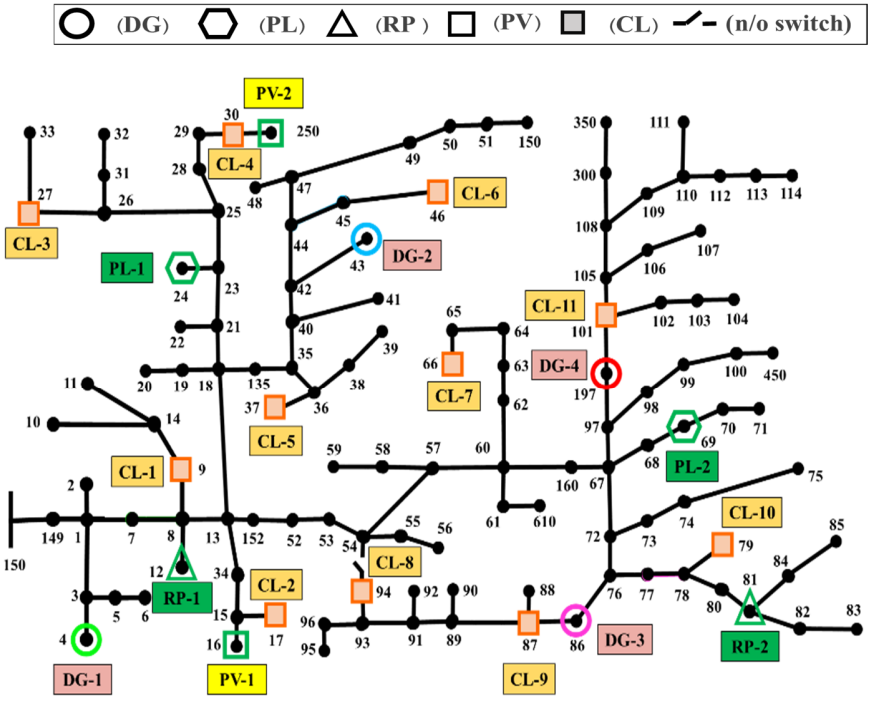

Fig. 6. IEEE 123-BUS with simulated resources and CLs

Table III: DGs parameters

DG	Bus	P_{max}(kW)	Q_{max}(kVar)	Capacity (kWh)
1	4	100	50	700
2	43	180	85	520
3	86	130	90	850
4	197	90	55	900

Table IV: PVs parameters

PV	Bus	Capacity (kVA)
1	16	100
2	250	80

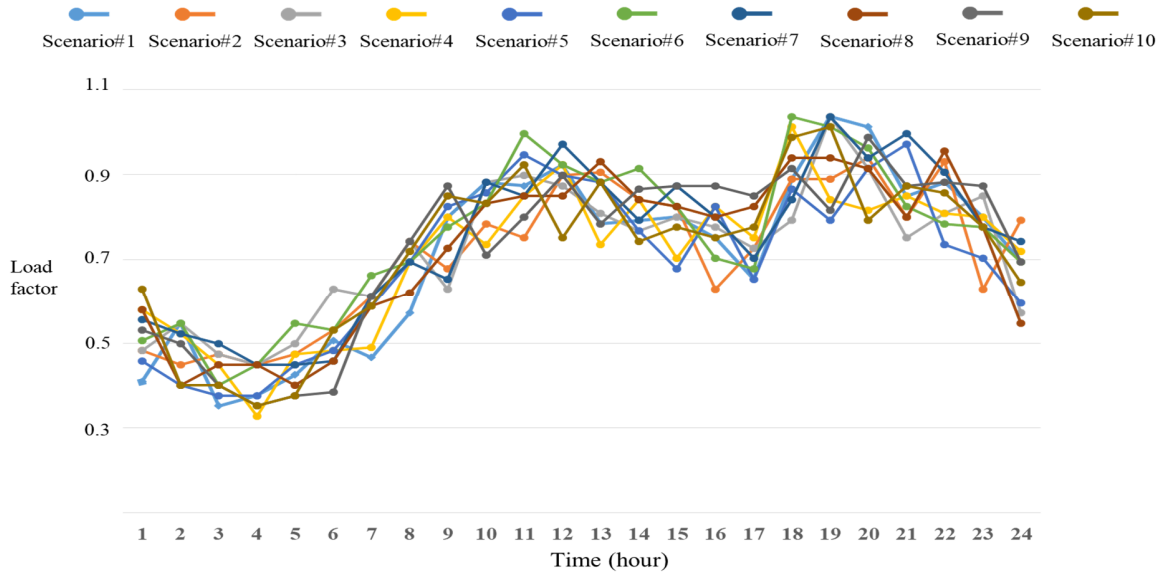

Fig. 7. Load factor profile in each scenario

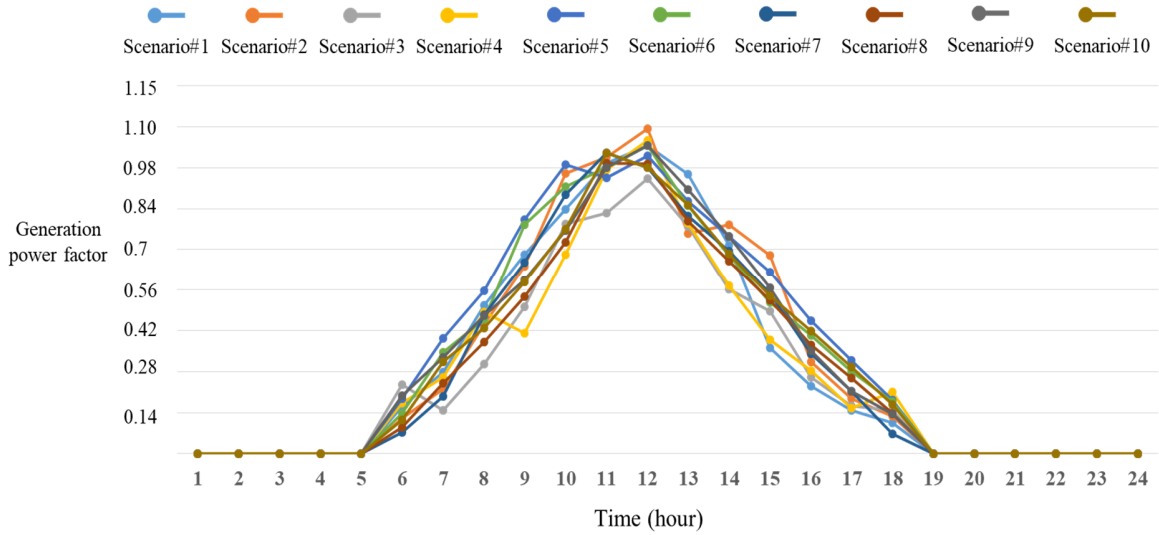

Fig. 8. Generation factor profile of the PVs in each scenario

Table V: Specification of the EVs, which participate in MG formation

EV Commercial brand ID	EV type	Discharge power (kW)	Battery capacity (kWh)	Gasoline tanker capacity (kg)	EG maximum generation power (kW)
1	BEV	6.6	62	-	-
2	BEV	11.5	79.5	-	-
3	BEV	7.2	60	-	-
4	PHEV	6.6	40	13	45
5	PHEV	7.2	38.3	18	45
6	BEV	11	100	-	-
7	BEV	11	50	-	-
8	BEV	11.5	62	-	-

Table VI: Coefficients of the linear piecewise function of the EGs power generation

a_1	a_2	a_3
-0.378	-0.756	-1.89

Case studies are designed as follows:

1. **Case Study 1:** In the first case, it is assumed that all parking lots and PV units are available to participate in the restoration of the CLs, and energy management of the EVs and other resources during outage are considered.
2. **Case Study 2:** In this case, the impact of the presence of each type of the EVs and the tie-switch on the amount of CLs by eliminating each of them has been investigated step by step.
3. **Case Study 3:** The third case study shows the assessment of the type of EVs charge/discharge scheduling before the outage and its impact on the amount of CLs restored.
4. **Case Study 4:** In this case, three scenarios are designed for evaluating the proposed approach in a real test system.

4.1 Case study 1

In this case, it is assumed that the incident happens at 4 pm, and the PDS is disconnected from the main grid. Therefore, the OMS have to restore CLs by forming several MGs. Consequently, by considering the condition of the distribution feeders, remote control switches and the availability of load control units and resources, several MGs are formed by opening/closing the switches. Fig. 9 shows the status of the formed MGs, and Fig. 10 and 11 show the scheduled power generation and consumption curves in MGs #3 and 4, respectively. As shown in Fig. 10, in MG #3, at the beginning of the restoration interval, most of the power generation is provided by the node in which the RPs are located. This is because some EVs that have been intended to depart from the RP and have been in the RP for a long time inject their surplus energy to the grid for CLs restoration. In the rest of the restoration interval three factors, such as DGs, EGs, and EV batteries,

contribute to restore the CLs. At the end of the restoration interval, the EVs' charge increases because the EVs' energy in the time of the departure needs to be higher than the minimum specified by their owner in the contract.

In MG #4, as can be seen in Fig. 11, supplying the CLs at the most of the power outage period is entirely done by DGs. As mentioned before, the start time of the event in this case is assumed 4 p.m. The behavior of the EVs in PL from 4 p.m onwards is such that they gradually leave the PL and as a result, the total available energy of the PL is reduced considerably. In this condition, a large part of the supplied CLs is provided by DGs. Moreover, at the beginning of the restoration interval, the high energy EVs that are going to departure from the PL is being discharged to supply part of the CLs along with the DG and to charge the EVs that are going to departure from the PL in the middle of the restoration interval. Also, The RI in this case is 0.83.

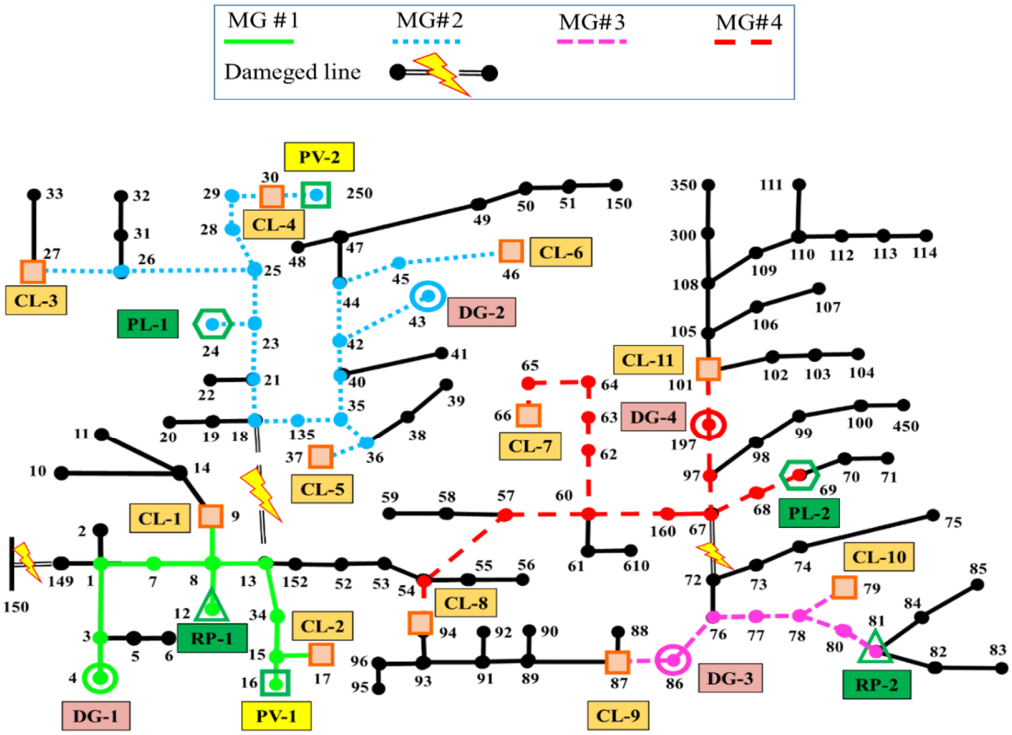

Fig. 9. MGs formation status in case study 1

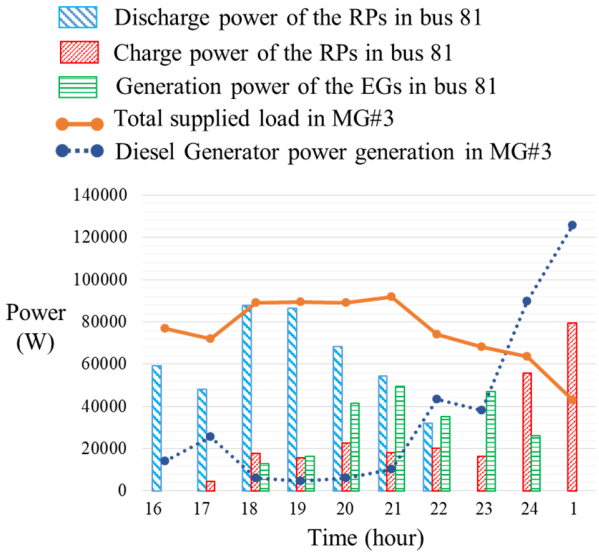

Fig. 10. Scheduled generation and consumption power curves in MG #3

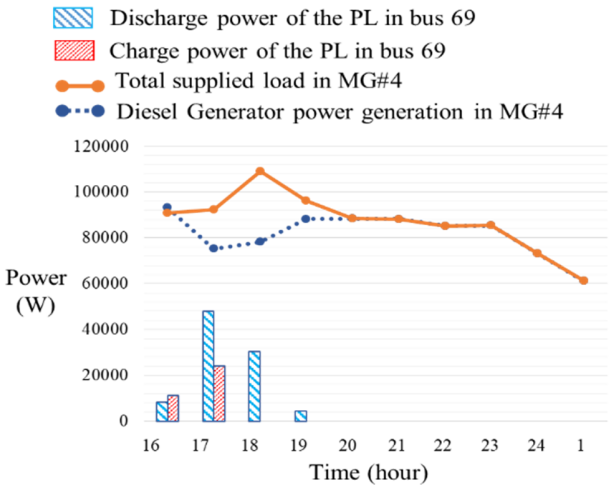

Fig. 11. Scheduled generation and consumption power curves in MG #4

4.2 Case study 2

In this section, the impact of the participation of different types of EVs, as well as the impact of tie-switches and demand response program on the amount of supplied load during the outage, is investigated. In this regard, five scenarios are designed: 1) restoration without the use of electrical energy of the EVs; 2) restoration with using just electrical energy of BEVs and PHEVs (without the use of fossil fuel of the PHEVs); 3), restoration without using any EVs; 4) restoration without the use of any EVs and tie-switches. 5) restoration without the use of any EVs, tie-switches and load control blocks. It should be noted that in all scenarios DGs are available for MG

formation. Fig.9 shows the MGs in scenario #1. The status of the formed MGs in scenario in scenarios #2 and #3 is shown in Fig. 12.

4.2.1 Scenario 1

In this scenario, it is assumed that no EVs (including BEVs and PHEVs) are allowed to use the electrical energy of their batteries. In this scenario, only PHEVs can use their fossil-fuel energy for participating in load restoration. Fig. 13 shows the scheduled amount of supplied loads in MG #2, which include PL, DG, and four CLs, in the two states of use and non-use of electrical energy of the EVs. As can be seen, the level of supplied energy when using batteries is higher than that of not using them. The numerical value of this advantage is about 384 kWh.

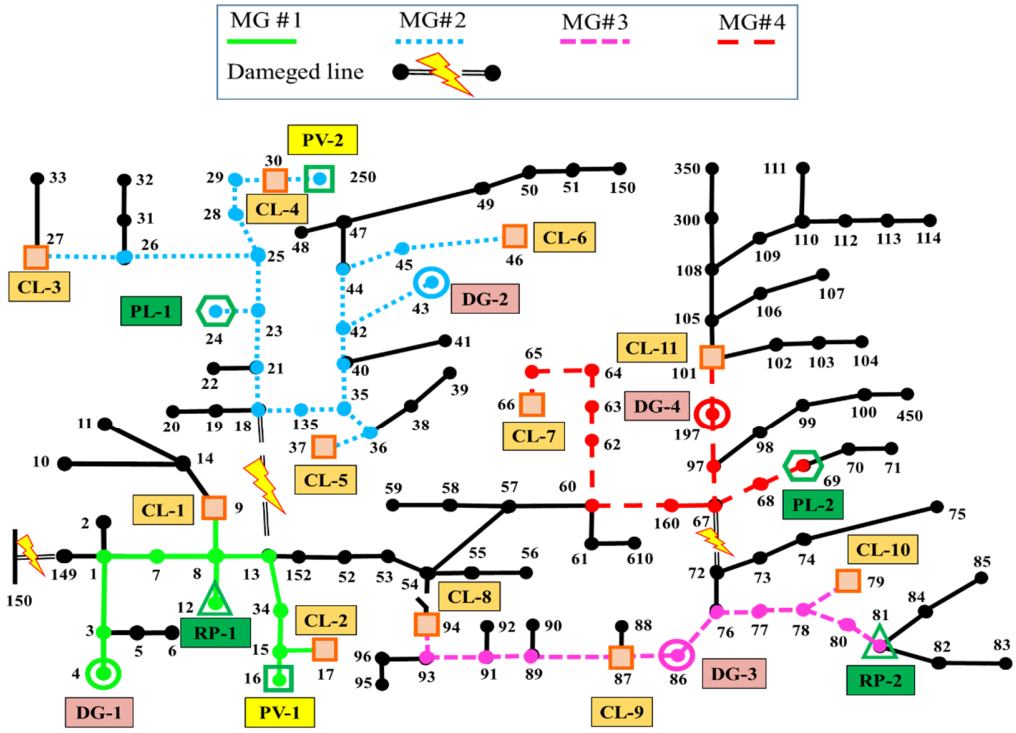

Fig. 12. MGs formation status in case study 2 and in scenarios 2 and 3

4.2.2 Scenario 2

Not using fossil-fuel energy by PHEVs in the load restoration is considered in this scenario. In this regard, the amount of energy generation by DG #2 in both the use and non-use of fossil fuel has been compared in Fig. 14. As can be seen, the scheduled amount of power generated and, therefore, the DG fuel consumption is significantly reduced when using EGs. In general, DGs are considered as master units in the grid; the optimal fuel consumption of these resources in the long-term outages is beneficial to the grid.

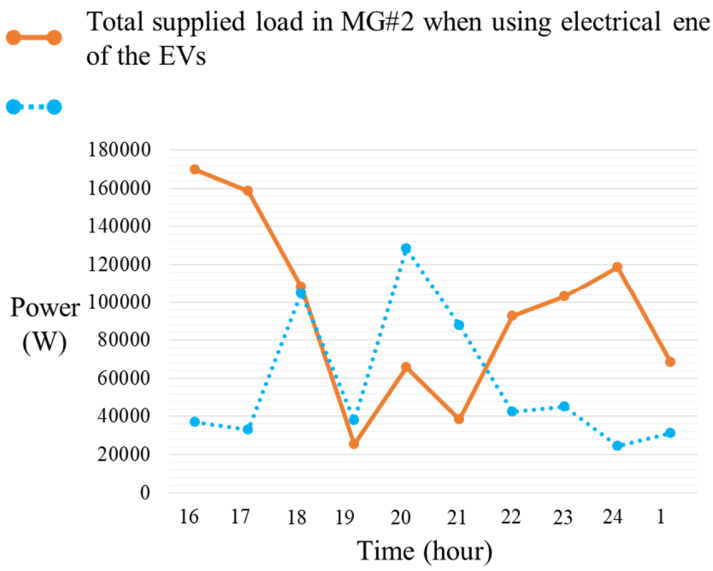

Fig. 13. Comparison of scheduled supplied load, when using or not using the battery of the EVs

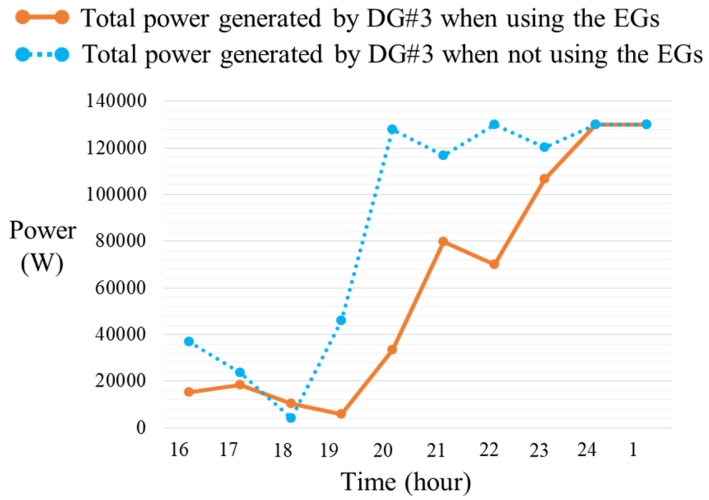

Fig. 14. Comparison of scheduled generation of DG, when using or not using the EGs

4.2.3 Scenario 3

In this scenario, due to the lack of appropriate control facilities it is assumed that none of the EVs (including BEVs and PHEVs) intend to participate in MG formation or they cannot be used in restoration. Therefore, the simulation is performed only in the presence of DGs. Fig. 15 shows the scheduled total supplied load in this scenario and the previous scenarios, which illustrates the significant impact of the EVs' participation on the amount of load restored after the outage.

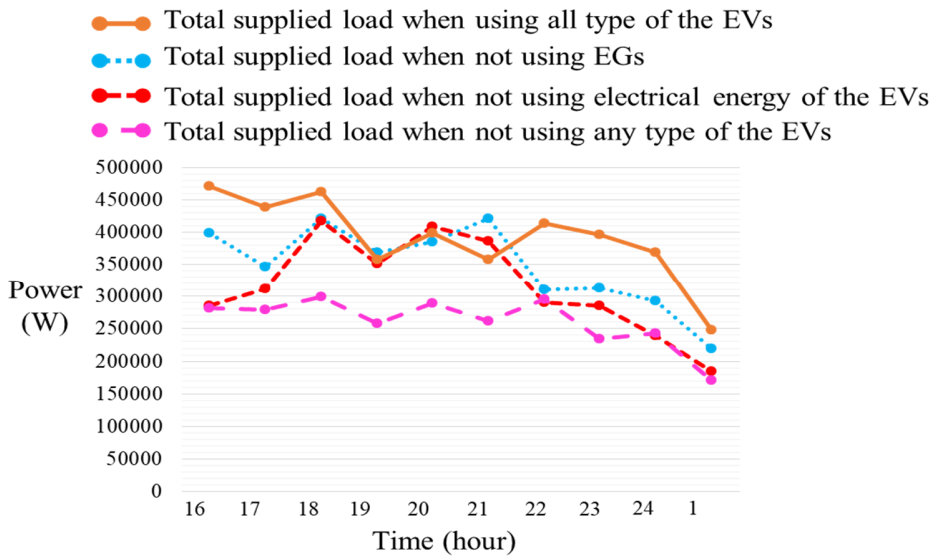

Fig. 15. Comparison of the supplied load in all designed scenarios

4.2.4 Scenario 4

In this scenario, in addition to not using the EVs, tie-switches are not used as well. Fig. 9 shows the status of the formation of MGs if the tie-switch is used, and Fig. 12 shows the status of the formation of the MGs if the tie-switch is not used. The difference between the two conditions is in the restoration of the CL #8. If the tie-switch is used, the energy supplied to the CL #8 will be increased by 52 kWh.

4.2.5 Scenario 5

In this scenario, it is assumed that the load control blocks are not available and the demand response program is not implemented after the formation of MGs. Fig. 12 shows the status of the formation of the MGs in this case. Moreover, Fig. 16 shows a comparison between different conditions in terms of RI. As shown in this figure, unlike the previous works, the use of all PDS capabilities, such as using EVs stored energy, tie-switches, master-slave control technique and load control facilities significantly increase the RI, and as a result, it improves the operational resilience of the distribution network.

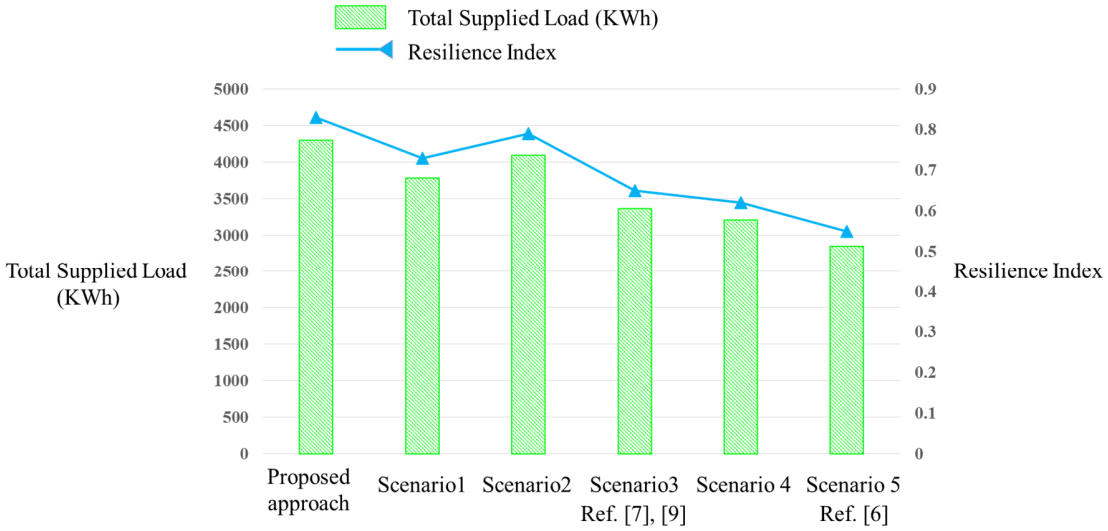

Fig. 16. Total supplied load and the resilience index in different conditions

4.3 Case study 3

In general, the type of charge/discharge scheduling before the outage can affect the amount of supplied load during the outage. For this purpose, three types of charge/discharge schedules are considered in this section to investigate the impact of each on the amount of supplied load. In the following, each of these plans is outlined. 1) Charging mode #1; in this mode, charge/discharge of EVs is based on the formulation presented in Section 2.1, and its purpose is to minimize costs. 2) Charging mode #2; in this mode, EVs are charged uniformly, depending on the time of their arrival and departure. 3) Charging mode #3; in this mode, EVs are charged at the maximum possible power without any control (this is done with considering the PLs or distribution substations limitation). The time of the outage, in this case, is considered 9 pm. Fig. 16 shows a comparison of the total amount of discharged power from RPs during the outage when using three charging modes employed before the outage.

As can be seen from Fig. 16, when using charging mode #1, due to the time of the outage, which is when the cost of the energy is high, the EVs have discharged most of their stored energy into the grid. Therefore, and their available energy for injecting into the grid at the time of outage is low. In charging modes #2 and #3, more energy is stored for injection due to the fact that EVs are not discharged in the hours before the outage begins. Comparing the two modes, as expected, the energy injected into the grid in the third mode is higher than in the second mode. The RI in this case and for three charging modes are 0.76, 0.84, and 0.91 respectively.

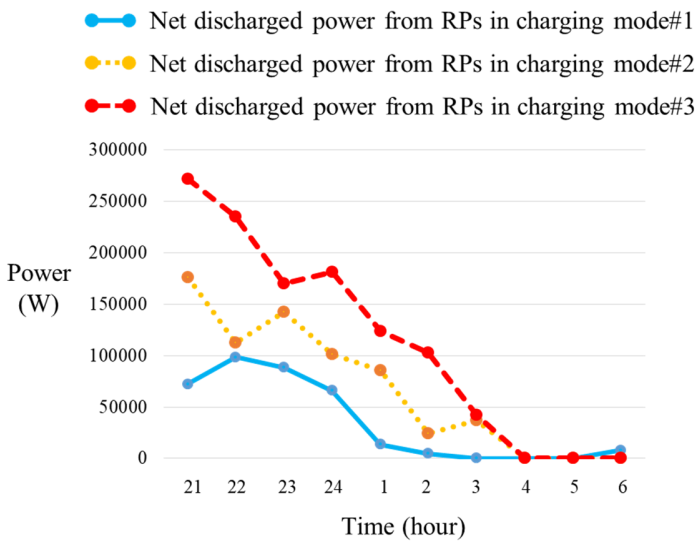

Fig. 16. Comparison of the discharged power of RPs in three charging mode

4.4 Case study 4

In this section, the proposed approach is implemented on a real 20 kV distribution network located in Sa'adat-Abad district of Tehran, Iran. The network consists of 492 buses, 516 feeders and 25 tie-switches. This network has one 63/20 kV substation that feeds 46.739 MW active and 15.063 MVAr reactive load. More details of this network are given in [31].18 DGs with a total capacity of 22.4 MW, 10 PLs with a total parking capacity of 300 cars (30 EVs for each PL) and 5 RPs with a total parking capacity of 50 cars (10 EVs for each RP) are added to this network. The failure state of the lines after the storm is assumed as [10], according to which 36 distribution lines are taken out of service. The outage duration is assumed to be 10 hours (between 14:00 and 23:00). The scheduled power generation and consumption curves are shown in Fig. 17 ad 18. As shown in Fig. 17, the participation of EVs in the early hours of restoration is high. The EVs that intend to leave the PL, by discharging their energy and charging other EVs, increase the participation time of the PLs. Three scenarios are designed for evaluating the proposed approach in this network: 1) restoration without the using of Master-Slave control technique (just DG units participate in the restoration); 2) restoration without the use of any type of EVs and tie-switches; 3) restoration with using the proposed approach (employing EVs, EGs and ti-switches). As shown in Fig. 17, by using the proposed approach, supplied load and consequently RI have increased.

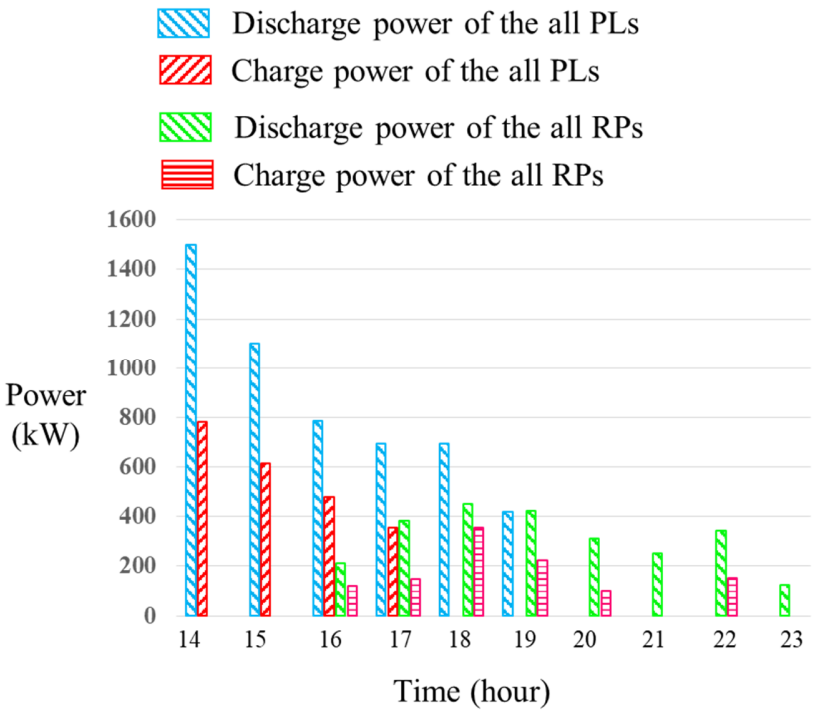

Fig. 17. Scheduled generation and consumption curves of the PLs and RPs in case study 4

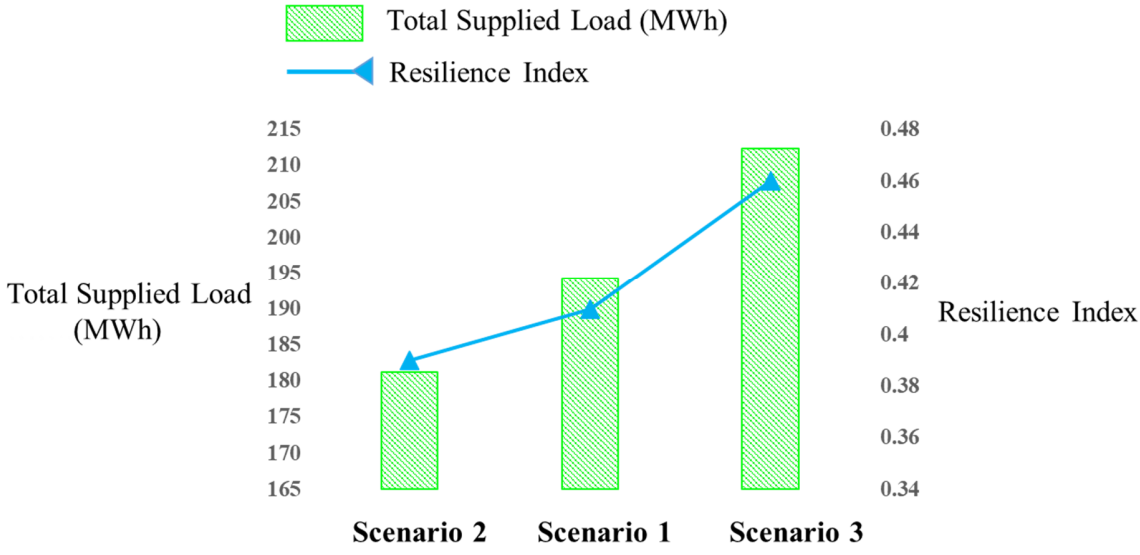

Fig. 18. Total supplied load and the resilience index in case study 4

5. Conclusions

This paper focused on enhancing the resilience of the PDS by restoring its CLs through the formation of several MGs and the participation of PHEVs and EVs. For the proper modeling of the problem with several parameters having uncertainty, a two-stage stochastic programming framework was proposed, and the uncertainties in the parameters of EVs, PV units and loads are modeled. Also, a novel method for load restoration in mesh networks has been proposed. Under the proposed method, the demand response program and master-slave control technique were employed to increase the supplied load by using several DERs in each MG, respectively. Various case studies were simulated to demonstrate the impact of factors, such as the participation of EVs, the existence of tie-switch, charge/discharge scheduling of the EVs before the outage, on the amount of supplied load. The simulation results show that the participation of EVs significantly increases the supplied load, and the use of a tie-switch in the PDS provided flexibility for path selection during the restoration of CLs, which also has a positive impact on the amount of supplied load. Moreover, proper charging / discharging scheduling of EVs before natural disasters can increase the supplied load during the outage period.

References

[1] A. Khodaei, "Resiliency-oriented microgrid optimal scheduling," *IEEE Trans. Smart Grid*, vol. 5, no. 4, pp. 1584–1591, 2014.

[2] R. Arghandeh *et al.*, "The Local Team: Leveraging Distributed Resources to Improve Resilience," *IEEE Power Energy Mag.*, vol. 12, no. 5, pp. 76–83, Sep. 2014.

[3] H. Farzin, M. Fotuhi-Firuzabad, and M. Moeini-Aghtaie, "Enhancing power system resilience through hierarchical outage management in multi-microgrids," *IEEE Trans. Smart Grid*, vol. 7, no. 6, pp. 2869–2879, 2016.

[4] A. Hussain, V.-H. Bui, and H.-M. Kim, "Optimal operation of hybrid microgrids for enhancing resiliency considering feasible islanding and survivability," *IET Renew. Power Gener.*, vol. 11, no. 6, pp. 846–857, 2017.

[5] A. Hussain, V.-H. Bui, and H.-M. Kim, "Resilience-Oriented Optimal Operation of Networked Hybrid Microgrids," *IEEE Trans. Smart Grid*, 2019.

[6] C. Chen, J. Wang, F. Qiu, and D. Zhao, "Resilient Distribution System by Microgrids Formation after Natural Disasters," *IEEE Trans. Smart Grid*, vol. 7, no. 2, pp. 958–966, 2016.

[7] S. Poudel and A. Dubey, "Critical Load Restoration Using Distributed Energy Resources for Resilient Power Distribution System," *IEEE Trans. Power Syst.*, vol. 34, no. 1, pp. 52–63, 2019.

[8] T. Ding, Y. Lin, Z. Bie, and C. Chen, "A resilient microgrid formation strategy for load restoration considering master-slave distributed generators and topology reconfiguration," *Appl. Energy*, vol. 199, pp. 205–216, 2017.

[9] K. S. A. Sedzro, X. Shi, A. J. Lamadrid, and L. F. Zuluaga, "A Heuristic Approach to the Post-disturbance and Stochastic Pre-disturbance Microgrid Formation Problem," *IEEE Transactions on Smart Grid*, vol. PP, no. c, p. 1, 2018, doi: 10.1109/TSG.2018.2887088.

[10] S. Mousavizadeh, M.-R. Haghifam, and M.-H. Shariatkhah, "A linear two-stage method for resiliency analysis in distribution systems considering renewable energy and demand response resources," *Appl. Energy*, vol. 211, pp. 443–460, 2018.

[11] K. B. Naceur and J. F. Gagn, "Global EV outlook 2017," *Int. Energy Agency Paris, Fr.*, 2017.

[12] K. Rahimi and B. Chowdhury, "A hybrid approach to improve the resiliency of the power distribution system," in *North American Power Symposium (NAPS), 2014*, 2014, pp. 1–6.

[13] K. Rahimi and M. Davoudi, "Electric vehicles for improving resilience of distribution systems," *Sustain. Cities Soc.*, vol. 36, pp. 246–256, 2018.

[14] H. Shin and R. Baldick, "Plug-in electric vehicle to home (V2H) operation under a grid outage," *IEEE Trans. Smart Grid*, vol. 8, no. 4, pp. 2032–2041, 2017.

[16] Liu, Z., Wang, D., Jia, H., Djilali, N., Zhang, W.: 'Aggregation and Bidirectional Charging Power Control of Plug-in Hybrid Electric Vehicles: Generation System Adequacy Analysis'*IEEE Trans. Sustain. Energy*, 2015, 6, (2), pp. 325–335.

[17] H. Farzin, M. Fotuhi-Firuzabad, and M. Moeini-Aghtaie, "Reliability Studies of Modern Distribution Systems Integrated With Renewable Generation and Parking Lots," *IEEE Trans. Sustain. Energy*, vol. 8, no. 1, pp. 431–440, 2017.

[18] K. V. Singh, H. O. Bansal, and D. Singh, "A comprehensive review on hybrid electric vehicles: architectures and components," *Journal of Modern Transportation*, vol. 27, no. 2, pp. 77–107, 2019.
[19] H. Haghighat, B. Zeng, "Distribution System Reconfiguration Under Uncertain Load and Renewable Generation," *IEEE Trans. Power Syst*., vol. 31 , pp. 2666 – 2675, 2016.
[15] A. Gholami, T. Shekari, F. Aminifar, and M. Shahidehpour, "Microgrid Scheduling with Uncertainty: The Quest for Resilience," *IEEE Trans. Smart Grid*, vol. 7, no. 6, pp. 2849–2858, 2016.
[21] M. Jacob, C. Neves, and D. Vukadinović Greetham, *Forecasting and Assessing Risk of Individual Electricity Peaks*. 2019.
[22] S. Mohammadi, S. Soleymani, and B. Mozafari, "Scenario-based stochastic operation management of MicroGrid including Wind, Photovoltaic, Micro-Turbine, Fuel Cell and Energy Storage Devices," *Int. J. Electr. Power Energy Syst.*, vol. 54, pp. 525–535, 2014.
[23] Tenti, P., Caldognetto, T.: 'Master/Slave Power-Based Control of Low-Voltage Microgrids' (Elsevier Inc., 2017)
[24] J. Y. Yen, "Finding the k shortest loopless paths in a network," *Management Science*, vol. 17, no. 11, pp. 712–716, 1971.
[25] P. M. Anagnostopoulos and S. A. Papathanassiou, "A Power Flow Method for Radial Distribution Feeders with DER Penetration," *Journal of Technology Innovations in Renewable Energy*, vol. 8, pp. 1–12, 2019.
[26] W. L. Winston, M. Venkataramanan, and J. B. Goldberg, *Introduction to mathematical .programming*, vol. 1. Thomson/Brooks/Cole Duxbury; Pacific Grove, CA, 2003.
[27] A. Abessi, A. Zakariazadeh, V. Vahidinasab, M. S. Ghazizadeh, and K. Mehran, "End-user participation in a collaborative distributed voltage control and demand response programme," *IET Gener. Transm. Distrib.*, vol. 12, no. 12, pp. 3079–3085, 2018.
[28] A. Kwasinski, V. Krishnamurthy, J. Song, and R. Sharma, "Availability evaluation of . micro-grids for resistant power supply during natural disasters," *IEEE Transactions on..Smart Grid,* vol. 3, no. 4, pp. 2007– 2018, 2012.
[29] S. Guner and A. Ozdemir, "Stochastic energy storage capacity model of EV parking lots," *IET Gener. Transm. Distrib.*, vol. 11, no. 7, pp. 1754–1761, 2017.
[30] NREL, System Advisor Model (SAM) 2012 [Online]. Available:https://sam.nrel.gov
[31] https://www.researchgate.net/publication/350670562_SaadatAbad_Distribution_Networks_Data?channel=doi&linkId=606cad04a6fdccf289fd43a0&showFulltext=true